The Plant Cell, Vol. 18, 3182–3200, November 2006, www.plantcell.org © 2006 American Society of Plant Biologists

Plant *N*-Glycan Processing Enzymes Employ Different Targeting Mechanisms for Their Spatial Arrangement along the Secretory Pathway [W][OA]

Claude Saint-Jore-Dupas,[a] Andreas Nebenführ,[b] Aurélia Boulaflous,[a] Marie-Laure Follet-Gueye,[a] Carole Plasson,[a] Chris Hawes,[c] Azeddine Driouich,[a] Loïc Faye,[a] and Véronique Gomord[a,1]

[a] Centre National de la Recherche Scientifique, Unité Mixte de Recherche 6037, IFRMP 23, GDR 2590, UFR des Sciences, Université de Rouen, 76821 Mont-Saint-Aignan Cedex, France

[b] Department of Biochemistry, Cellular, and Molecular Biology, University of Tennessee, Knoxville, Tennessee 37996-0840

[c] School of Biological and Molecular Sciences, Oxford Brookes University, Oxford OX3 0BP, United Kingdom

The processing of *N*-linked oligosaccharides in the secretory pathway requires the sequential action of a number of glycosidases and glycosyltransferases. We studied the spatial distribution of several type II membrane-bound enzymes from *Glycine max*, *Arabidopsis thaliana*, and *Nicotiana tabacum*. Glucosidase I (GCSI) localized to the endoplasmic reticulum (ER), α-1,2 mannosidase I (ManI) and *N*-acetylglucosaminyltransferase I (GNTI) both targeted to the ER and Golgi, and β-1,2 xylosyltransferase localized exclusively to Golgi stacks, corresponding to the order of expected function. ManI deletion constructs revealed that the ManI transmembrane domain (TMD) contains all necessary targeting information. Likewise, GNTI truncations showed that this could apply to other type II enzymes. A green fluorescent protein chimera with ManI TMD, lengthened by duplicating its last seven amino acids, localized exclusively to the Golgi and colocalized with a *trans*-Golgi marker (ST52-mRFP), suggesting roles for protein–lipid interactions in ManI targeting. However, the TMD lengths of other plant glycosylation enzymes indicate that this mechanism cannot apply to all enzymes in the pathway. In fact, removal of the first 11 amino acids of the GCSI cytoplasmic tail resulted in relocalization from the ER to the Golgi, suggesting a targeting mechanism relying on protein–protein interactions. We conclude that the localization of *N*-glycan processing enzymes corresponds to an assembly line in the early secretory pathway and depends on both TMD length and signals in the cytoplasmic tail.

INTRODUCTION

The plant Golgi apparatus consists of individual stacks of membrane bound flattened cisternae surrounded by small vesicles that are dispersed throughout the cytoplasm (Staehelin and Moore, 1995; Driouich and Staehelin, 1997; Andreeva et al., 1998; Dupree and Sherrier, 1998). The number of Golgi stacks per cell and the number of cisternae per stack vary with the plant species and the cell type, reflecting the physiological conditions, the developmental stage, and the functional requirements of a plant cell (reviewed in Staehelin and Moore, 1995; Andreeva et al., 1998). Despite these variations, each individual Golgi stack can be described as a polarized structure with its cisternal morphology and its enzymatic activities changing gradually from the endoplasmic reticulum (ER)-adjacent *cis*-face to the *trans*-face (Fitchette et al., 1999).

The Golgi apparatus is not only a central sorting point of the secretory pathway (Nebenführ, 2002; Hawes, 2005; Hawes and Satiat-Jeunemaitre, 2005), but this compartment also provides the central biosynthetic function of a complex carbohydrate factory (Driouich and Staehelin, 1997; Nebenführ and Staehelin, 2001). Thus, the Golgi is the site of maturation of *N*-glycans on glycoproteins, *O*-glycosylation of Hyp-rich glycoproteins and arabinogalactan proteins, and de novo synthesis of cell wall matrix polysaccharides, such as hemicelluloses and pectins. These biosynthetic processes are performed by glycosidases and glycosyltransferases (Lerouge et al., 1998; Saint-Jore-Dupas et al., 2004).

During the maturation of *N*-glycans, ER and Golgi-localized glycosidases trim sugar residues from an oligosaccharide precursor of *N*-glycans to a $Man_5GlcNAc_2$ structure. Subsequently, Golgi-localized glycosyltransferases mediate the transfer of sugar residues from nucleotide sugar donors onto the *N*-glycans. In mammalian cells, it has been shown that glycosidases and glycosyltransferases are distributed along the Golgi from the *cis*- to the *trans*-regions in the order in which they process *N*-glycans; however, there is some overlap and variation in their distribution depending on the cell type (Roth, 1991; Nilsson et al., 1993a; Velasco et al., 1993; Rabouille et al., 1995; Idgoura et al., 1999). With the exception of α-glucosidase II (Trombetta et al., 1996,

[1] To whom correspondence should be addressed. E-mail vgomord@crihan.fr; fax 33-2-35-14-67-87.

The authors responsible for distribution of materials integral to the findings presented in this article in accordance with the policy described in the Instructions for Authors (www.plantcell.org) are: Andreas Nebenführ (nebenfuehr@utk.edu) and Véronique Gomord (vgomord@crihan.fr).

[W] Online version contains Web-only data.

[OA] Open Access articles can be viewed online without a subscription.

www.plantcell.org/cgi/doi/10.1105/tpc.105.036400

2001; P. Soussilane, C. Saint-Jore-Dupas, and V. Gomord, unpublished data), which is a soluble heterodimer, glycosidases and glycosyltransferases responsible for the *N*-glycan maturation are type II membrane proteins with a short N-terminal cytoplasmic tail (CT), a single transmembrane domain (TMD), a stem region (S), and a large catalytic domain associated with the enzyme activity. In mammalian cells, Golgi retention of glycosyltransferases has been attributed to the TMD with variable contributions of the cytoplasmic and lumenal domains depending on the protein (reviewed in Colley, 1997; Gleeson, 1998; Munro, 1998; Zerfaoui et al., 2002). Various models have been proposed to explain the retention of glycosyltransferases in the mammalian Golgi. The kin recognition model proposes that the resident proteins form large hetero-oligomers by protein–protein interaction in the Golgi membrane and are consequently prevented from entering the budding vesicles destined to another compartment (Nilsson et al., 1993b, 1994, 1996; Opat et al., 2000; Qian et al., 2001). According to the lipid bilayer model, the fit between the length of TMD and the thickness of the lipid bilayer of each organelle membrane determines the localization because the membrane of each organelle has its specific lipid components (Munro, 1991, 1995a; Bretscher and Munro, 1993). The third model proposes that the CT of glycosyltransferases plays a key role in their specific localization to the Golgi (Osman et al., 1996; Milland et al., 2001, 2002).

This article illustrates an attempt at elucidating the targeting domain(s), allowing the selective retention of glycosyltransferases in certain cisternae of the plant Golgi apparatus. The main reason for the absence of data available in this field is that the first plant Golgi enzymes were cloned only recently (Essl et al., 1999; Nebenführ et al., 1999; Strasser et al., 1999, 2006; Boisson et al., 2001; Dirnberger et al., 2002; Pagny et al., 2003). To date, only 10 cDNA encoding *Arabidopsis thaliana* enzymes involved in *N*-glycan maturation and eight cDNA involved in cell wall polysaccharides biosynthesis have been cloned and the corresponding protein characterized, while ~420 genes encoding enzymes implicated in glycoconjugate biosynthesis and potentially located in the Golgi have been identified in the *Arabidopsis* genome (Coutinho et al., 2003). This also explains why the first evidence for a subcompartmentation of *N*-glycosylation enzymes in the plant Golgi was obtained using an indirect approach based on immunolocalization of glycosyltransferase products (Lainé et al., 1991; Fitchette et al., 1994, 1999). In this way, it was shown that β-1,2-xylose is added onto plant *N*-glycans mainly in the medial Golgi, whereas α-1,3-fucosylation occurs predominantly in the *trans*-side of Golgi (Fitchette et al., 1994). Moreover, the biosynthesis of Lewis-a antenna constitutive of plant complex *N*-glycans is a late Golgi event taking place in the *trans*-Golgi and the *trans*-Golgi network (Fitchette et al., 1999). A similar method was also used to show subcompartmentation within the Golgi of glycosyltransferases involved in the assembly of cell wall polysaccharides (Zhang and Staehelin, 1992). Finally, another indirect approach based on the expression of heterologous glycosyltransferases, such as rat α-2,6-sialyltransferase (α-2, 6-ST), in plant cells has provided data suggesting that similar subcompartmentation signals might be conserved between plant and animal Golgi type II membrane proteins (Boevink et al., 1998; Wee et al., 1998).

With the recent cloning of plant glycosyltransferases, data on their localization were obtained by expression of these enzymes as fusions with a green fluorescent protein (GFP). For instance, it was shown that the N-terminal 77 amino acids of the tobacco (*Nicotiana tabacum*) *N*-acetylglucosaminyltransferase I (GNTI; Essl et al., 1999) or the N-terminal 92 amino acids of the *Arabidopsis* mannosidase II (MANII; Strasser et al., 2006), including the CT and TMD of both maturation enzymes, are sufficient to target GFP to the Golgi of *Nicotiana benthamiana* leaf epidermal cells. Similarly, the N-terminal 35 amino acids of *Arabidopsis* β-1, 2-xylosyltansferase (XYLT) were fused to GFP and the recombinant protein expressed in tobacco BY-2 suspension-cultured cells (Dirnberger et al., 2002; Pagny et al., 2003). In both studies, it was proposed that the CT and the TMD contain the information sufficient for Golgi targeting, and the fusion protein was shown to be concentrated in the medial Golgi cisternae (Pagny et al., 2003).

All studies mentioned above point to a central role of the CT and TMD for proper localization of *N*-glycan processing enzymes; however, no systematic study of a type II membrane protein targeting in the early secretory pathway of plant cells has been published to date. Herein, we demonstrate that TMD length is a major determinant for localization of soybean (*Glycine max*) α-1,2 mannosidase I (ManI) to the *cis*-half of the Golgi and to the ER and that an increase in the length of its TMD relocates this type II membrane protein further downstream to the *trans*-half of the Golgi consistent with the lipid bilayer thickness model. By contrast, in silico analyses performed on cloned glycosylation enzymes illustrate that the TMD length is not sufficient by itself to explain the compartmentation of all *N*-glycan processing enzymes as illustrated here for glucosidase I (GCSI) where the CT is crucial for ER retention.

RESULTS

Early Golgi Type II Membrane Proteins Are Partially Located in the ER

To better understand the mechanisms allowing the selective retention of *N*-glycan processing enzymes in the early Golgi compartments, the localization of a series of GFP fusions to four different members of the *N*-glycan processing machinery (GCSI, ManI, GNTI, and XYLT; Figure 1) was studied after stable expression in tobacco BY-2 cells. Fluorescence of a full-length ManI-GFP fusion construct was detected by confocal laser scanning microscopy in small bodies (Figures 2A and 2B) that moved through the cytoplasm as it has been described previously for this construct in another independent cell line (Nebenführ et al., 1999). In addition, a substantial fluorescence signal was observed in a reticulate network throughout the cytoplasm that was indistinguishable from the ER network stained by a GFP-HDEL construct (Figures 2D and 2E). To check if ER labeling was due to overexpression of the recombinant proteins, BY-2 cells expressing ManI-GFP were incubated with the protein synthesis inhibitor cycloheximide. After 2 h of treatment, the targeting pattern remained unchanged, showing that the steady state location of ManI-GFP is the Golgi and the ER (cf. Figures 2B and 2C).

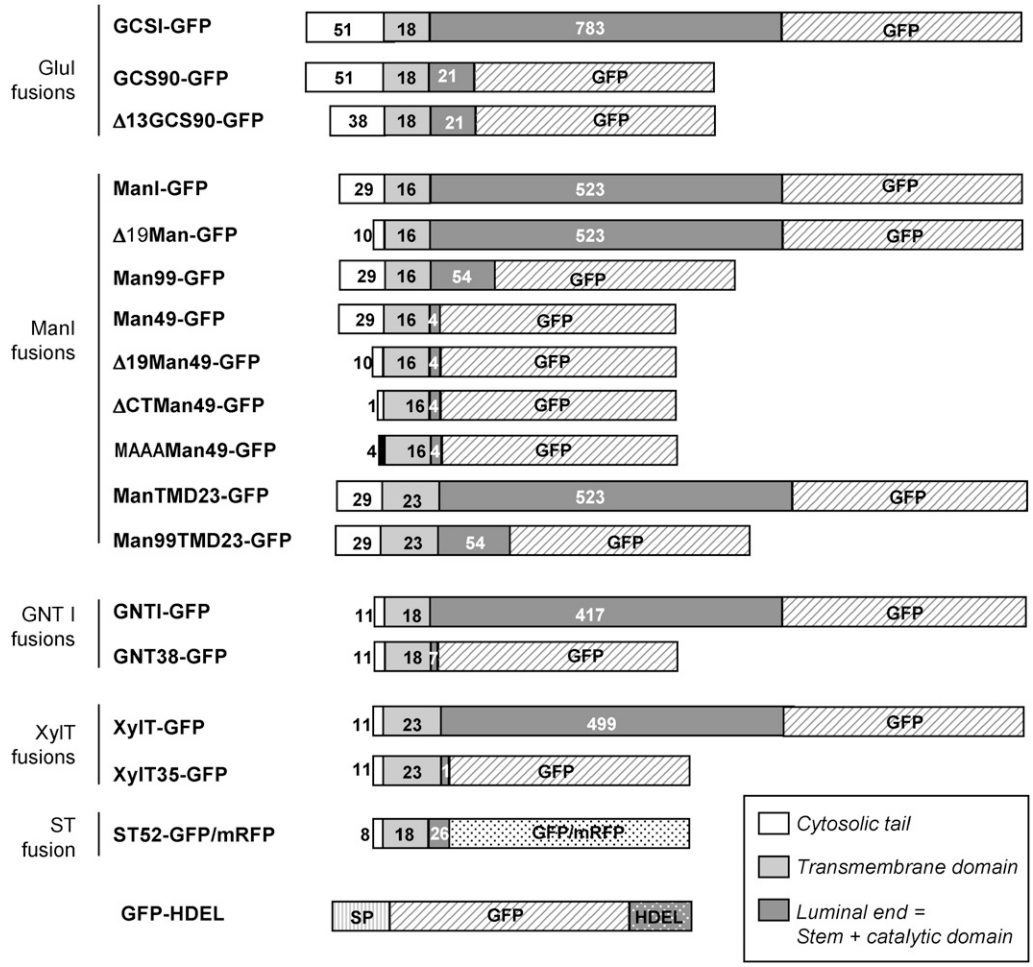

Figure 1. Schematic Representation of Fusion Proteins Analyzed in This Study.

GCSI-GFP: full-length *Arabidopsis* GCSI fused to GFP. GCS90-GFP: the first 90 N-terminal amino acids of GCSI fused to GFP. Δ13GCS90-GFP: GCS90-GFP minus the first 13 N-terminal amino acids. ManI-GFP: full-length *G. max* ManI fused to GFP. Δ19Man-GFP: ManI-GFP minus the first 19 N-terminal amino acids. Man99-GFP and Man49-GFP: the first 99 and 49 amino acids of ManI, respectively, fused to GFP. Δ19Man49-GFP: Man49-GFP minus the first 19 N-terminal amino acids. ΔCTMan49-GFP: the whole CT was deleted from Man49-GFP. MAAAMan49-GFP: the CT of Man49-GFP was replaced by an artificial CT containing three Ala residues. ManTMD23-GFP and Man99TMD23-GFP: ManI-GFP and Man99-GFP, respectively, where the TMD was lengthened from 16 to 23 amino acids. GNTI-GFP: full-length *N. tabacum* GNTI fused to GFP. GNT38-GFP: the first 38 N-terminal amino acids of GNTI fused to GFP. XylT-GFP: full-length *Arabidopsis* XYLT fused to GFP. XylT35-GFP: the first 35 amino acids of XYLT fused to GFP. ST52-GFP/mRFP: the first 52 amino acids of a rat α-2,6-ST fused to mRFP. GFP-HDEL: a GFP version containing the sporamine signal peptide and a C-terminal HDEL ER retention sequence.

To confirm that fluorescent spots were Golgi stacks, the cells were treated for 2 h with 50 $\mu g \cdot mL^{-1}$ of brefeldin A (BFA). This BFA treatment caused the green spots to disappear, and the cortical and transvascular ER became more fluorescent (cf. Figure 2F to Figures 2B and 2E) as has been described previously for several Golgi-localized GFP fusion proteins expressed in tobacco leaf epidermis and BY-2 suspension-cultured cells (Ritzenthaler et al., 2002; Saint-Jore et al., 2002).

To compare the location of ManI to one of the other plant *N*-glycosylation enzymes in the secretory pathway, we analyzed under the same conditions the subcellular localization of *N*-glycan maturation enzymes acting before, just after ManI, or much later. The first enzyme we studied was *Arabidopsis* GCSI. This type II membrane protein trims the first sugar residue from the precursor oligosaccharide in the ER immediately after its attachment to the nascent glycoprotein (see a schematic representation of plant *N*-glycan maturation in Figure 11 and additional data in Supplemental Table 1 online). The full-length protein (Boisson et al., 2001) was fused to GFP and, consistent with what was shown for human GCSI in COS cells (Hardt et al., 2003), the fusion protein was exclusively located in the ER in BY-2 cells (Figure 2G).

The second candidate investigated was GNTI from *N. tabacum* (Strasser et al., 1999). This glycosyltransferase adds a first *N*-acetylglucosamine residue on *N*-glycans soon after ManI has removed an α-1,2-mannose (Figure 11). The full-length protein

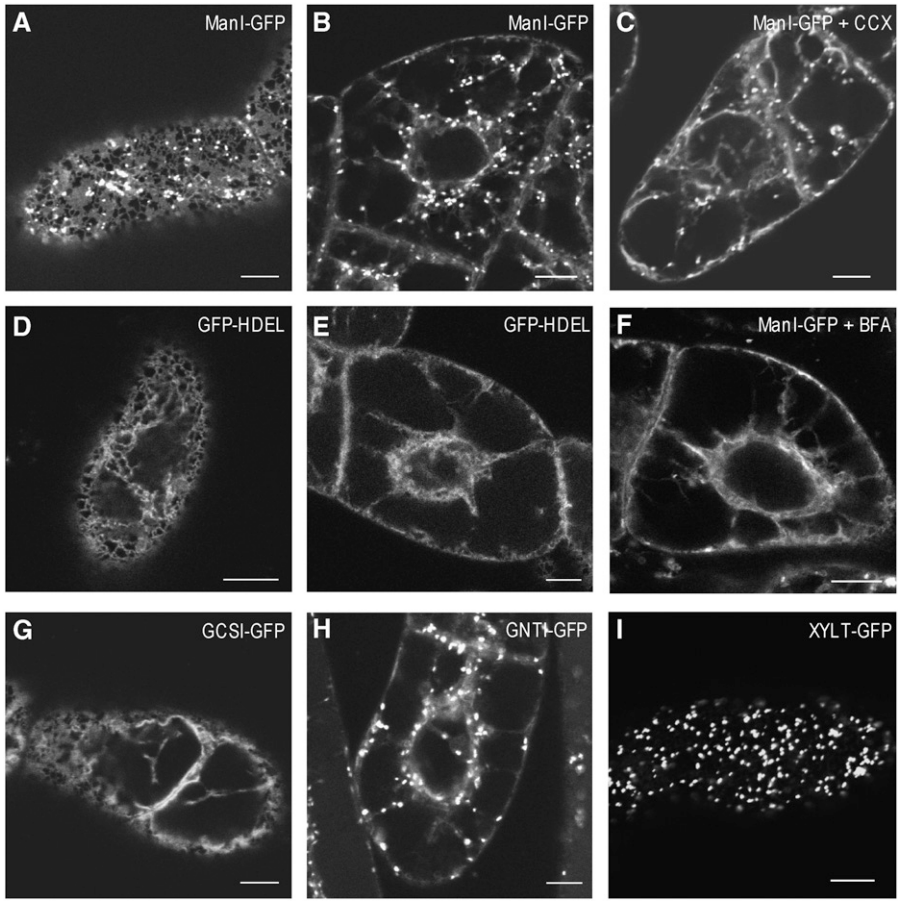

Figure 2. ManI-GFP and GNTI-GFP Are Located to the Golgi and to the ER, whereas GCSI-GFP Is Exclusively Accumulated in the ER and XYLT-GFP in the Golgi.

Transgenic BY-2 tobacco cell lines were analyzed 3 to 4 d after subculturing. Bars = 8 μm.

(A) and **(B)** ManI-GFP is located to the Golgi and to the ER (**[A]**, cortical view; **[B]**, cross section where ER labeling around the nucleus and in the vacuolar strands is characteristic).

(C) After a 2-h treatment with the protein synthesis inhibitor cycloheximide, ER and Golgi labeling observed with ManI-GFP fusion remained unchanged, showing that the steady state localization of ManI-GFP is the Golgi and the ER.

(D) and **(E)** GFP-HDEL highlights the ER.

(F) After a 2-h treatment with BFA (50 mg·mL^{-1}), fluorescent Golgi stacks have disappeared, while ER fluorescence is increased due to the relocation of ManI-GFP.

(G) GCSI-GFP is an ER resident membrane protein and shows a similar fluorescence pattern as GFP-HDEL **(D)**.

(H) GNTI-GFP is targeted to the Golgi and to the ER as observed for ManI-GFP **(B)**.

(I) XYLT-GFP accumulates exclusively in Golgi stacks.

was fused to GFP, and GNTI-GFP was expressed in tobacco BY-2 suspension-cultured cells. Interestingly, the steady state location of the fusion was the Golgi and the ER (Figure 2H) in a pattern very similar to ManI-GFP (cf. Figures 2B and 2H). These data strongly suggest that the *N*-glycan processing enzymes considered to act very early in the Golgi apparatus, such as ManI and GNTI, are targeted to the Golgi but also to the ER in tobacco BY-2 suspension-cultured cells.

Finally, the third candidate, XYLT from *Arabidopsis*, was located in the Golgi only (Figure 2I), confirming the results from Pagny et al. (2003), who demonstrated that the N-terminal end of this enzyme targets GFP to a medial subset of cisternae of Golgi stacks.

To ascertain whether protein expression levels might alter localization of our fusion proteins, we have confirmed these results in different independent cell lines expressing the fusion proteins, at least 3 months after transformation. Imaging of cells was always performed on the third or fourth day after subculturing, which corresponds to the optimal growth phase under our culture conditions. Nevertheless, to further validate that ER labeling was not due to overexpression of the fusion, we have controlled for each fusion that the labeling pattern was unchanged after a 2-h treatment with cycloheximide. Additional data illustrating that translation is indeed blocked under these conditions are available online. Protein gel blots revealed with

anti-GFP antibodies and the enhanced chemiluminescence staining have shown a very low signal over background for the recombinant proteins, indicating a low level of expression for all fusion proteins in this study (data not shown). Further evidence for a level of fusion protein expression compatible with a functional nonsaturated secretory pathway was obtained from coexpression experiments when ManI-GFP is located both in the ER and Golgi in the same cell, while a Golgi marker (ST52-mRFP) is found exclusively in the Golgi (Figures 4A to 4C). All together, results obtained under these carefully controlled conditions clearly show that *N*-glycosylation enzymes are targeted specifically to the ER (GCSI) or to the Golgi (XYLT) exclusively, but some enzymes have a dual steady state location in both organelles, as is the case for ManI, GNTI (this study), and other membrane proteins, such as prolyl 4-hydroxylase (Yuasa et al., 2005) and ERD2 (Boevink et al., 1998; Saint-Jore et al., 2002). In a next step, we decided to investigate which signals were responsible for the targeting of the population of glycosylation enzymes showing a dual steady state distribution Golgi/ER.

The Luminal Domain Is Not Necessary for Golgi and ER Targeting of ManI and GNTI

Recent studies regarding the specific Golgi retention of the three plant glycosylation enzymes GNTI, XYLT, and *Arabidopsis* ManII (Figure 11) indicate that their specific targeting is mediated by signals contained in their N-terminal part, including the CT, the TMD, and the stem for GNTI (Essl et al., 1999; Dirnberger et al., 2002; Pagny et al., 2003; Strasser et al., 2006). Here, we have investigated the role of the luminal domain in the targeting of ManI and GNTI.

To determine if the portion of ManI located in the Golgi lumen plays a role in the targeting of this glycosidase to the Golgi and the ER membranes, the first 99 amino acids (CT+TMD+S) or the first 49 amino acids (CT+TMD) of ManI were fused to GFP, and the corresponding chimeric proteins were named Man99-GFP and Man49-GFP, respectively (Figure 1). Man99-GFP and Man49-GFP were either stably expressed in BY-2 suspension-cultured cells or transiently expressed in tobacco leaf epidermal cells by leaf infiltration. Both Man99-GFP and Man49-GFP chimeric proteins were observed in the Golgi and in the ER in both expression systems (Figures 3A, 3B, and 3D to 3F), exactly as previously observed for the full-length construct (Figures 2A and 2B). It is important to note that when these truncated fusions were transiently expressed in tobacco leaves, the ER labeling was still observed 5 d after transformation when the overall expression levels are already strongly declining (Figure 3F), whereas XYLT35-GFP was located in the Golgi only (Pagny et al., 2003; Figure 3I). This further confirms that the partial location of the ManI fusions in the ER is not due to overexpression of the chimeric proteins. In addition, when BY-2 cells expressing Man99-GFP were treated with the protein synthesis inhibitor cycloheximide for 2 h, the ER labeling did not disappear (Figure 3C) as had been observed for the full-length fusion (cf. Figure 2C).

To get a better understanding of where the fusion proteins are localized within the Golgi stacks, ManI-GFP was coexpressed with the *trans*-Golgi marker ST52-mRFP, which is derived from ST52-GFP (Saint-Jore et al., 2002; Runions et al., 2006) by replacing GFP with the monomeric red fluorescent protein (mRFP; Campbell et al., 2002). When the two chimeric proteins were expressed simultaneously in BY-2 cells, in contrast with ManI-GFP, ST52-mRFP was not detected in the ER, and both fluorescence signals were observed in Golgi bodies but did not perfectly colocalize (Figures 4A to 4C). These results are consistent with previous studies that have demonstrated that (1) the ManI-GFP fusion is located in the *cis*-half of the Golgi in BY-2 cells (Nebenführ et al., 1999), and (2) the 52 N-terminal amino acids of rat α-2,6-ST are sufficient to target a reporter protein predominantly to the *trans*-half of Golgi stacks (Boevink et al., 1998). Thus, confocal microscopy is sufficient to illustrate that ManI-GFP and ST52-mRFP accumulate in a different subset of cisternae in the Golgi apparatus. Finally, when, Man99-GFP or Man49-GFP was coexpressed with the *trans*-Golgi marker ST52-mRFP, the two fluophores only partially overlapped (Figures 4D to 4I), suggesting that the intra-Golgi localization of the truncated fusion proteins was the same as that of the full-length fusion ManI-GFP.

The first 77 N-terminal amino acids of the tobacco GNTI, including the CT, the TMD, and the stem, were previously described to contain the information required to maintain Golgi retention of this glycosyltransferase (Essl et al., 1999). This polypeptide domain fused to GFP has been shown to be preferentially located in the Golgi, but the chimeric protein was also detected in the ER as observed here for the full-length construct (Figure 2H).To determine if the sequence remaining in the Golgi lumen is involved in the Golgi and ER targeting of GNTI, the lumenal part (39 amino acids) was removed and the remaining first 38 N-terminal amino acids (CT+TMD) of this glycosyltransferase were fused to GFP (Figure 1). The fusion protein was named GNT38-GFP and stably expressed in BY-2 suspension-cultured cells or transiently in tobacco leaf epidermal cells. In both expression systems, GNT38-GFP was located in the Golgi and in the ER (Figures 3G and 3H) as previously observed for the full-length construct (GNTI-GFP; Figure 2H). In addition, when GNT38-GFP was stably coexpressed with ST52-mRFP in BY-2 cells, as observed before with Man99-GFP and Man49-GFP, the two fluorescent spots overlapped, but some red fluorescence was distinguishable from the yellow, suggesting that GNT38-GFP is not in the *trans*-Golgi (Figures 4J to 4L) as previously observed for ManI.

It is clear from these results that the CT and TMD of both ManI and GNTI are sufficient to target these glycosylation enzymes to their steady state location: the ER and the early Golgi compartments. By contrast, the same domain (CT+TMD) targets XYLT35-GFP to the Golgi only, both in BY-2 cells (Pagny et al., 2003) and *N. tabacum* leaf epidermal cells (Figure 3I).

The CT Is Not Necessary for the Retention of ManI in the Early Compartments of the Secretory Pathway

The N-terminal cytosolic region of many membrane-bound proteins residing in the mammalian and yeast ER and/or in the Golgi apparatus contains signals that facilitate either their retrieval from the Golgi back to the ER (Teasdale and Jackson, 1996; Zerangue et al., 1999) or their export from the ER to the Golgi (Giraudo and Maccioni, 2003). In plants, the length of CTs can vary widely between the different glycosidases and glycosyltransferases

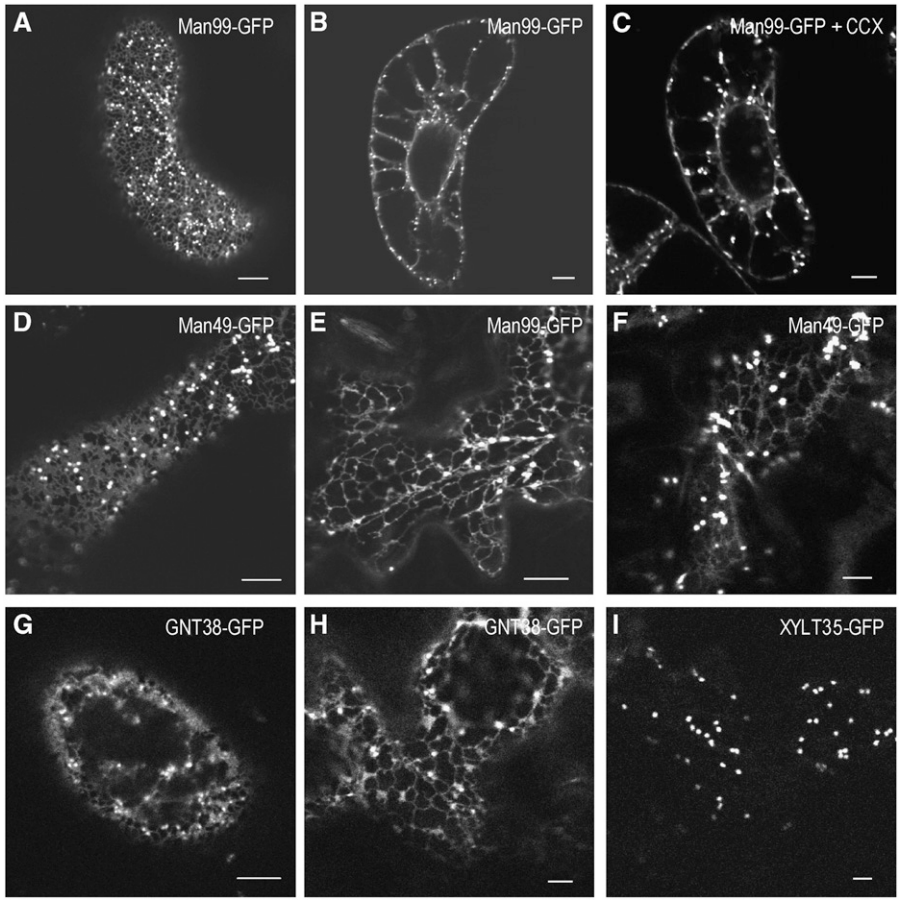

Figure 3. Luminal Domains Are Not Necessary to Target ManI and GNTI to the Golgi and the ER.

(A) and **(B)** Cells expressing Man99-GFP display a punctuate and network pattern of GFP fluorescence typical of the organization of Golgi stacks and cortical ER in BY-2 cells and similar to the labeling observed for ManI-GFP.
(C) The ER and Golgi labeling remains unchanged when cells expressing Man99-GFP were incubated with the protein synthesis inhibitor cycloheximide for 2 h.
(D) Man49-GFP was located to the Golgi and to the ER in BY-2 suspension-cultured cells.
(E) and **(F)** Leaf epidermal cells expressing Man99-GFP **(E)** and Man49-GFP **(F)** display the same labeling pattern 5 d after agroinfiltration as BY-2 cells expressing the same proteins.
(G) and **(H)** As observed for the truncated forms of ManI fused to GFP, GNT38-GFP was located to the Golgi and to the ER in BY-2 suspension-cultured cells **(G)** and in *Nicotiana* leaf epidermal cells **(H)**.
(I) XYLT35-GFP highlights only the Golgi in *Nicotiana* leaf epidermal cells.
Bars = 8 μm.

(Figure 11). For instance, GCSI and ManI contain a long CT (51 and 29 amino acids, respectively). In comparison, the CTs of GNTI and XYLT are only composed of 11 amino acids.

To define more precisely the targeting signal of ManI and to investigate the role of the relatively long cytoplasmic domain (29 amino acids) of this glycosidase in this targeting, we generated two fusion proteins (Δ19Man-GFP and Δ19Man49-GFP). In the latter two proteins, 19 amino acids were removed so that the CT was shortened down to 10 amino acids, like the CTs of XYLT and GNTI. This truncation removed a potential dibasic motif (KxR) that might function in ER-to-Golgi transport (Giraudo and Maccioni, 2003), although another potential ER export signal remained. A complete removal of the CT was attempted (ΔCTMan49-GFP, Figure 1), but it was not possible to get this fusion protein expressed in tobacco cells. To look for a targeting determinant in the remaining 10 amino acids of the CT, the CT sequence was substituted by an artificial sequence (MAAA) (MAAAMan49-GFP, Figure 1). This artificial sequence does not contain any known targeting sequences and does not affect the length of the hydrophobic TMD.

The three constructs (MAAAMan49-GFP, Δ19Man-GFP, and Δ19Man49-GFP) were expressed in tobacco cells. The two latter labeled the ER and the Golgi (Figures 5A to 5D) just like the constructs from which they originate (Figures 2A, 2B, 3D, and 3F). In addition, the fusion protein containing an artificial MAAA CT was located in the same compartments (Figure 5E), indicating

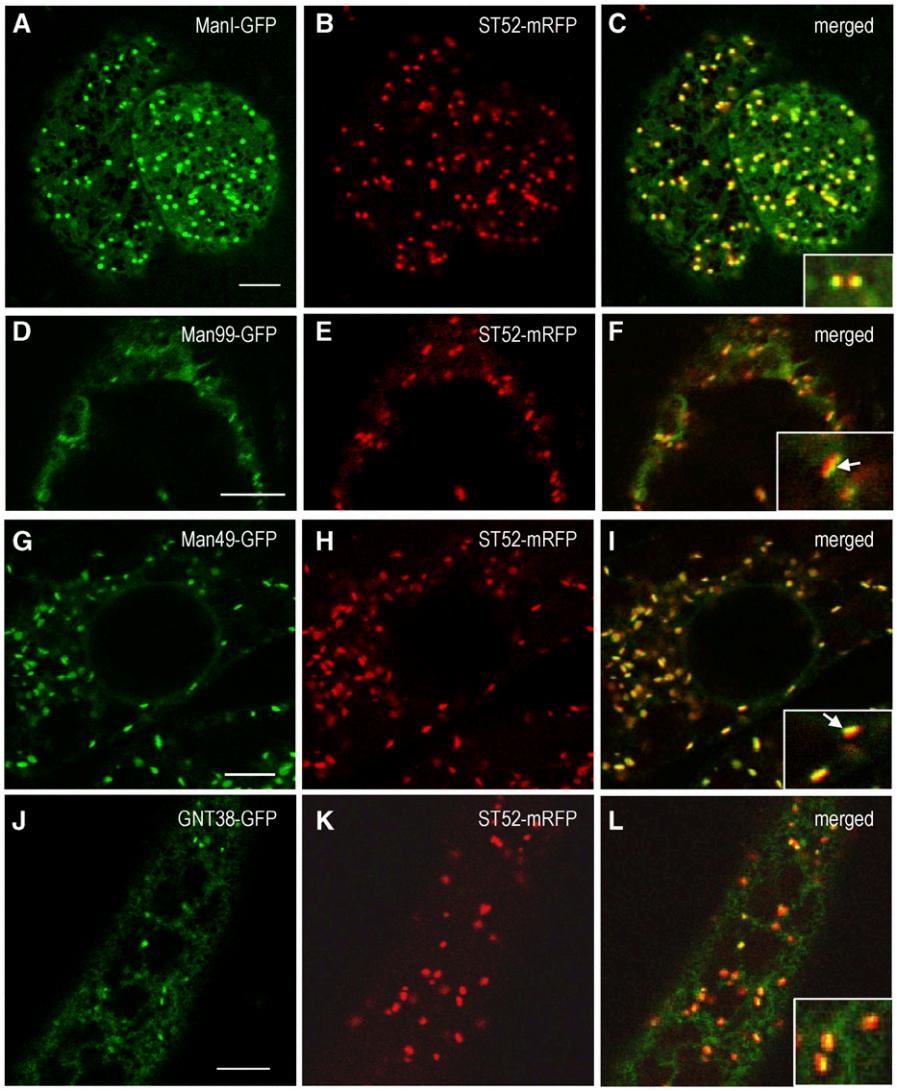

Figure 4. ManI and GNTI Fusions Accumulate into the Early Golgi.

Transgenic cell lines coexpressing ST52-mRFP (**[B]**, **[E]**, **[H]**, and **[K]**) and ManI-GFP **(A)**, Man99-GFP **(D)**, Man49-GFP **(G)**, or GNT38-GFP **(J)** in BY-2 suspension-cultured cells and corresponding merged images (**[C]**, **[F]**, **[I]**, and **[L]**). Insets: magnification of selected Golgi stacks (2.2× zoom). Note that stacks often appear tricolored (arrows in **[F]** and **[I]**) with the GFP fusions on one side (green), the ST52-RFP on the other side (red), and a region of overlap between them (yellow). This suggests that all the GFP constructs localize to the *cis*-Golgi as had been shown previously for ManI-GFP (Nebenführ et al., 1999), whereas ST52-RFP is in the *trans*-Golgi (Boevink et al., 1998).
Bars = 8 μm in **(A)** to **(I)** and 16 μm in **(J)** to **(L)**.

that the N-terminal cytosolic region is not necessary for ManI targeting; consequently, all information required for its steady state localization to both the ER and the Golgi apparatus is contained within the 20 amino acids of the MAAAMan49-GFP construct (i.e., in the TMD and C-terminal flanking amino acids).

TMD Length Plays the Key Role in Golgi Targeting and Subcompartmentation of ManI

According to the membrane thickness model, the distribution of *N*-glycan maturation enzymes in the secretory pathway is based on the length of their TMDs (Bretscher and Munro, 1993). The membranes of the secretory pathway organelles increase in thickness from the ER to the plasma membrane. The ER and the *cis*-Golgi membranes are only 4 to 5 nm thick, whereas the membranes of the *trans*-Golgi, the secretory vesicles, and the plasma membrane are 8 to 9.5 nm thick (Grove et al., 1968; Morré and Mollenhauer, 1974). Moreover, targeting related to TMD length was previously illustrated by studying the location of reporter proteins after varying the length of their TMD in animal systems (Munro, 1991, 1995a, 1995b) and, for type I proteins, also in plant cells (Brandizzi et al., 2002a). This implies that the

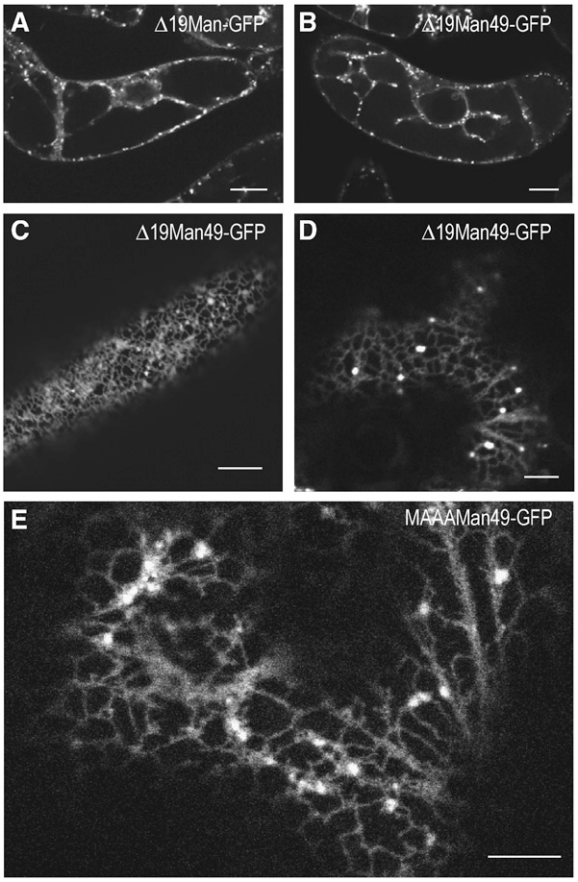

Figure 5. The CT Is Not Needed for ManI Localization to the Golgi and the ER.

(A) to **(C)** Δ19Man-GFP **(A)** and Δ19Man49-GFP (**[B]** and **[C]**) are located to the Golgi and to the ER in BY-2 suspension-cultured cells. Bars = 16 μm.

(D) Δ19Man49-GFP also highlights the Golgi and the ER in *Nicotiana* leaf epidermal cells.

(E) A similar distribution pattern was observed for MAAAMan49-GFP after expression of this fusion in leaf epidermal cells.

Bars = 8 μm.

membrane of a specific compartment can only accommodate hydrophobic TMDs of the matching length.

In this study, we have shown that the information required for ManI targeting is contained within a 20–amino acid sequence, including the 16–amino acid TMD. To investigate whether the length of the TMD could play a key role in the targeting of this type II membrane protein in the early plant secretory pathway, we designed two fusion proteins, ManTMD23-GFP and Man99TMD23-GFP, where the TMD of ManI was lengthened from 16 to 23 amino acids by duplication of its last seven amino acids (Figure 1). ManTMD23-GFP and Man99TMD23-GFP were expressed in BY-2 suspension-cultured cells and in tobacco leaf epidermal cells. In both plant expression systems, ManTMD23-GFP and Man99TMD23-GFP were exclusively located in bright spots (Figures 6A, 6B, and 6D) and were sensitive to the fungal toxin BFA (50 $\mu g \cdot mL^{-1}$, 2 h; Figure 6C). The expression patterns of ManTMD23-GFP and Man99TMD23-GFP were similar to either the XYLT-GFP fusion (Figures 3I and 6E) or the ST52-mRFP fusion (Figure 6F), both located exclusively in the Golgi in BY-2 suspension-cultured cells and tobacco leaf epidermal cells, as has been confirmed previously by electron microscopy (Boevink et al., 1998; Pagny et al., 2003).

Similar results were obtained in other plant systems used for transient expression. Indeed, Man99-GFP was located in the Golgi and in the ER in soybean (Figure 6G) and in tomato (*Solanum lycopersicum*) leaf epidermal cells (Figure 6I), whereas Man99TMD23-GFP was found almost exclusively in the Golgi in both expression systems (Figures 6H and 6J).

To further investigate the subcompartmentation of ManTMD23-GFP and Man99TMD23-GFP, stable BY-2 suspension-cultured cells coexpressing one or the other of these GFP fusions and ST52-mRFP were established. In the merged images, it was impossible to separate green spots from red spots, suggesting that the GFP fusions containing a 23–amino acid TMD have moved forward within the Golgi toward the *trans*-face so that they colocalize with ST52-mRFP at the confocal level (cf. Figures 4 and 7). Interestingly, the spot patterns were similar in cortical images (Figures 7D to 7F) compared with cross sections (Figures 7G to 7I), reinforcing the assumption that the Man-GFP fusions with a longer TMD and the *trans*-Golgi marker ST52-mRFP perfectly colocalize. By contrast, the medial Golgi marker (XYLT35-GFP) and the *trans*-Golgi marker (ST52-mRFP) resulted in fluorescent spots that did not overlap perfectly in the merged image (Figures 7J to 7L).

Electron microscopy coupled to immunogold labeling with polyclonal anti-GFP antibodies allowed us to determine more precisely the intra-Golgi localization of these fusion proteins. As illustrated in Figure 8, the Man99-GFP fusion accumulated mainly to the *cis*-side of the Golgi (Figure 8B), whereas the Man99TMD23-GFP fusions are principally localized to the *trans*-side of the Golgi (Figure 8C). Similar results were obtained with ManI-GFP and ManTMD23-GFP (data not shown). Control experiments using the preimmune serum or wild-type tobacco BY-2 suspension-cultured cells showed no or very little nonspecific Golgi labeling (Figure 8A).

In conclusion, together, these results indicate that TMD length plays a key role in the targeting of ManI to the ER and the *cis*-Golgi compartments, and an increase in the length of the TMD from 16 to 23 amino acids relocates this type II membrane protein further downstream toward the *trans*-face of the Golgi (Figure 8D).

Late and Early Golgi Proteins Redistribute in the ER in the Presence of BFA

Taking advantage of the large panel of Golgi marker generated during this study, we have investigated the possibility that Golgi proteins located in different Golgi subcompartments may behave differently after BFA treatment. Cells expressing ER-soluble or membrane markers (GFP-HDEL or GCS90-GFP, Figures 9A to 9D), the ER/early Golgi marker (Δ19Man49-GFP, Figures 9E and 9F), the medial Golgi marker (XYLT35-GFP, Figures 9G and 9H), or the late Golgi marker (Man99TMD23-GFP or ST52-mRFP,

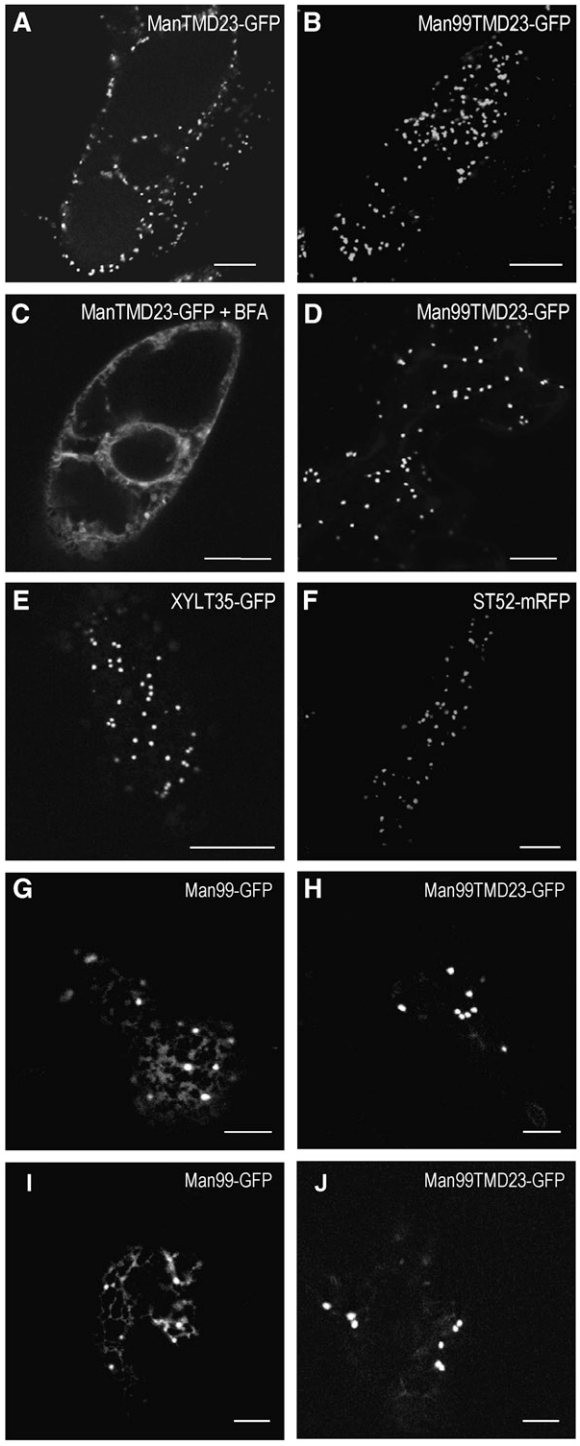

Figure 6. An Increase in TMD Length Displaces ManI from the ER to the Golgi.

Modification of TMD length in ManTMD23-GFP **(A)** and Man99TMD23-GFP **(B)** leads to the accumulation of fusion proteins in the Golgi of BY-2 tobacco cells, as observed for XYLT35-GFP **(E)** and ST52-mRFP **(F)**. No ER labeling was observed in cells expressing these fusion proteins. The same results were obtained after transient expression in *Nicotiana* **(D)**, *G. max* (**[G]** and **[H]**), or *S. lycopersicum* (**[I]** and **[J]**) leaf epidermal cells. ManTMD23-GFP is redistributed to the ER after a 2-h treatment with BFA **(C)**. Bars = 16 μm.

Figures 9I to 9L) were treated with BFA (50 $\mu g \cdot mL^{-1}$) for 2 h. At the end of the BFA treatment, all the fusion proteins accumulated in bright aggregates and in the ER (Figures 9E to 9L) except for the ER markers that were never found in aggregates (Figures 9A to 9D). We illustrate here that all markers relocated in the ER in presence of BFA. In cells coexpressing ER/early Golgi or late Golgi proteins with ST52-mRFP, BFA induces the redistribution of both markers into the ER and into Golgi aggregates (Figure 10), except for GFP-HDEL (Figures 10A to 10F) and GCS90-GFP (Figure 9D) that were not found in the aggregates. In some cases, there are subtle differences in timing, but these are not trivial to detect and also not informative with respect to intra-Golgi localization. Furthermore, no significant difference was observed in the fluorescence patterns observed after BFA treatment of cells expressing either a soluble (GFP-HDEL) or a membrane protein (GCS90-GFP) marker (Figures 9A to 9D).

The TMD Length Model Does Not Apply to All Type II Membrane Proteins

To determine whether the TMD length could be the only Golgi sorting determinant allowing the subcompartmentation of all glycosidases and glycosyltransferases along the plant secretory system, we compared the N-terminal sequences of characterized glycosylation enzymes (Figure 11). This analysis is hampered by the small number of sequences of different enzymes cloned and functionally characterized from a single species as well as a still smaller number of electron microscopy data to correlate TMD lengths and membrane thickness in a single plant system. In silico analysis of the N-terminal sequence (CT+TMD) of all plant glycosylation enzymes cloned so far clearly shows a trend for longer TMDs in proteins with the most downstream location in the Golgi stacks (Figure 11). For instance, it is interesting to note that none of the enzymes that are supposed to be located in the late Golgi, such as α-1,3-fucosyltransferases and α-1,4-fucosyltransferases, have a TMD shorter than 20 amino acids. These results are confirmed when the MENSAT_V1,8, PHOBIUS, or PRED_TMR programs are used for TMD length prediction (see Supplemental Table 2 online). However, exceptions to this general trend can be noticed when similar glycosylation enzymes from different species are compared, for example, the ManI TMDs ranging from 16 (soybean) to 20 amino acids (*Arabidopsis*).

Based on its short 18–amino acid TMD that could perfectly fit with the lipid bilayer model to explain its localization in the ER membrane, we have selected GCSI to check for general applicability of this model. To define whether the TMD of GCSI was sufficient for its targeting and retention in the ER, we first deleted most of the luminal part of this glycosidase (containing the catalytic domain) and fused its first N-terminal 90 amino acids (CT+TMD+S) to GFP to get the fusion protein GCS90-GFP (Figure 1). When this fusion was expressed in tobacco cells, the ER was highlighted (Figures 12A and 12B) in a pattern very similar

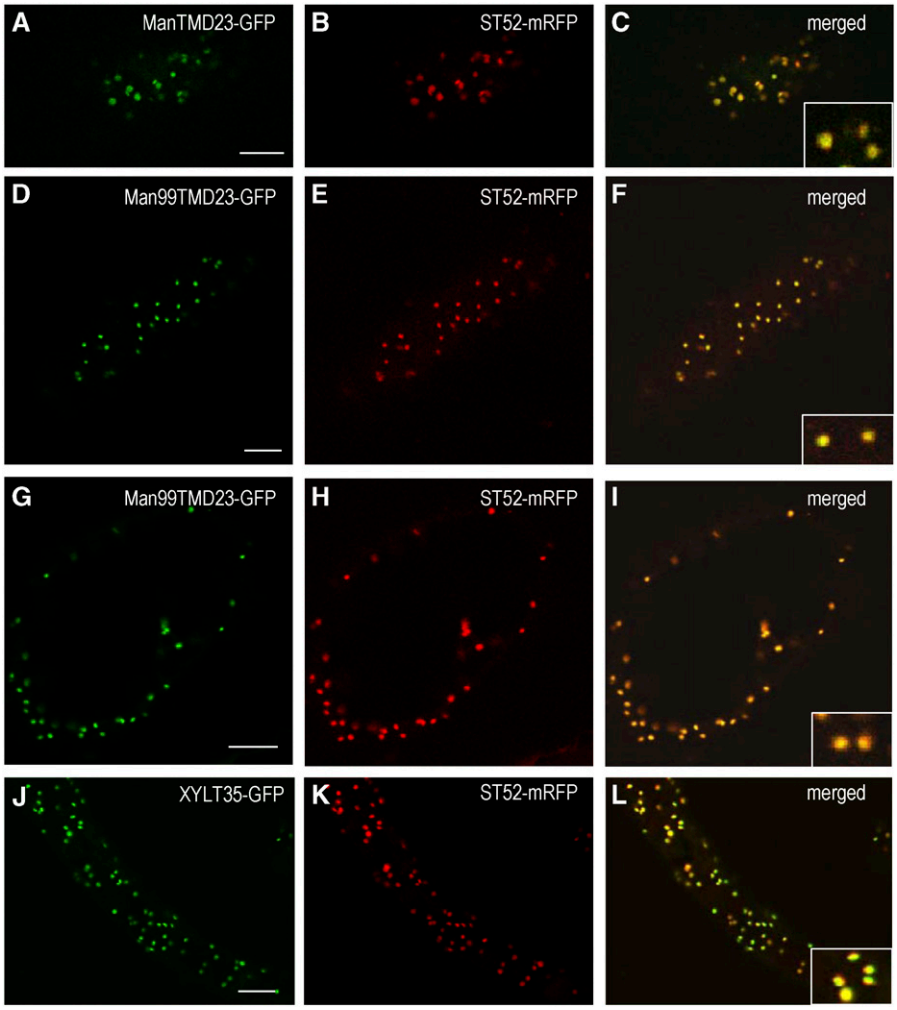

Figure 7. An increase in TMD Length Displaces ManI and Man99 to Late Golgi Compartments: Evidence from Coexpression with the *trans*-Golgi Marker ST52-mRFP.

(A) to **(C)** When ManTMD23-GFP **(A)** and ST52-mRFP **(B)** were coexpressed in BY-2 suspension-cultured tobacco cells, they both targeted to the Golgi and perfectly colocalized, as illustrated in the zoomed insets (2.2×) where the spots are yellow.
(D) to **(I)** When Man99TMD23-GFP and ST52-mRFP were coexpressed in BY-2 suspension-cultured cells, they both targeted to the Golgi and perfectly colocalized (2.2× zoomed insets). In the cross sections (**[G]** to **[I]**), some red fluorescence can be distinguished from the yellow, whereas it is almost impossible in the cortical section, suggesting that the Golgi stacks are oriented toward the plasma membrane in the cortical cytoplasm.
(J) to **(L)** XYLT35-GFP and ST52-mRFP were coexpressed in BY-2 suspension-cultured cells. Both fusion proteins targeted to the Golgi, but some green fluorescence can be distinguished from the yellow in some cases, consistent with their localization mainly in the medial Golgi (XYLT35-GFP) or in the *trans*-Golgi (ST52-mRFP).
Bars = 8 μm.

to the one obtained with the full-length construct GCSI-GFP and the GFP-HDEL construct (cf. micrographs in Figures 12A and 12B to Figures 2D, 2E, 2G, and 10C). This result clearly shows that GCSI targeting to the ER depends on signals located within the CT, the TMD, and/or the 21 luminal amino acids remaining in this truncated protein. In a further attempt at defining the minimal protein sequence required for localization of GCSI in the ER, we deleted the first N-terminal 13 amino acids from the GCS90-GFP construct to obtain Δ13GCS90-GFP (Figure 1). When this fusion was expressed in tobacco suspension-cultured or leaf epidermal cells, the chimeric protein was located exclusively in Golgi-like spots (Figures 12D and 12E), as observed for XYLT-GFP (Figures 3I and 6E) and ST52-GFP (Figure 12F). In conclusion, the 18–amino acid long TMD of GCSI is not sufficient to target this glycosidase in the ER membrane, and additional information contained in the first 13 amino acids of the CT is required for the normal localization of this glycosylation enzyme in the secretory system. This result provides experimental proof that factors other than TMD length can influence the positioning of glycosylation enzymes in the early secretory pathway.

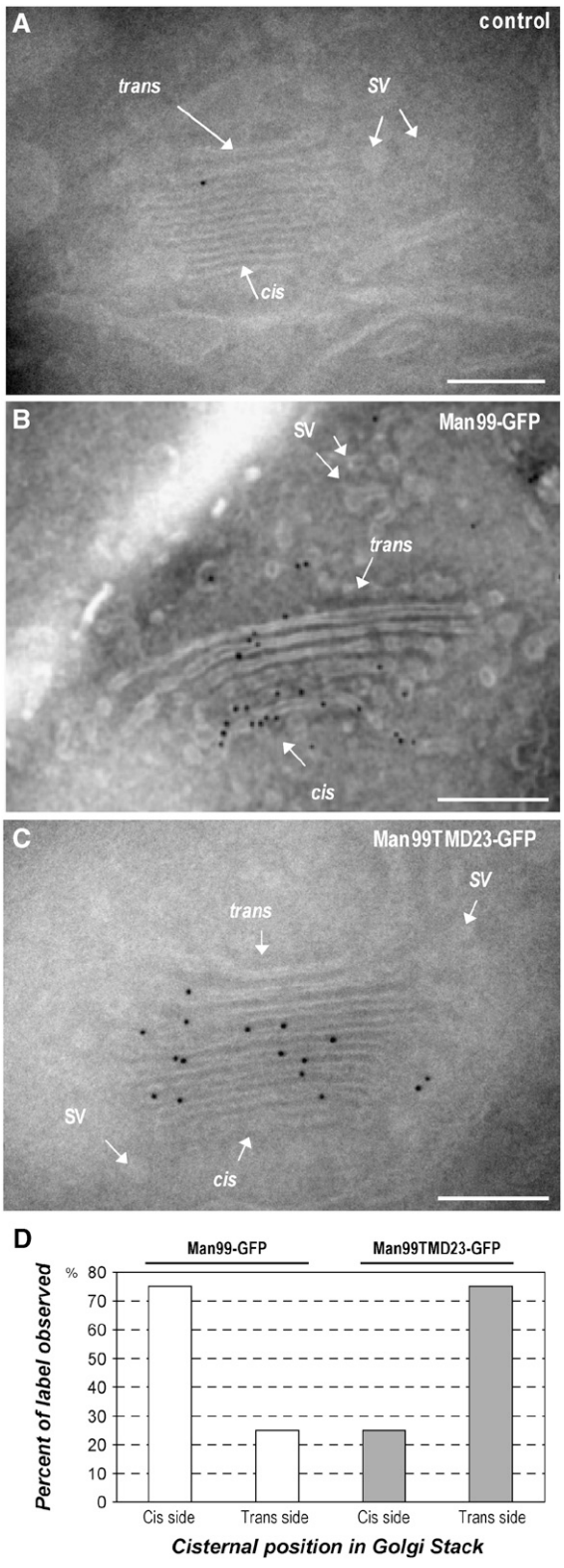

Figure 8. Subcompartmentation of Man99-GFP and Man99TMD23-GFP in the Golgi Apparatus.

Electron micrographs of Golgi stacks were realized from suspension-cultured wild-type BY-2 tobacco cells **(A)** or from BY-2 cells expressing Man99-GFP **(B)** or Man99TMD23-GFP **(C)**. Immunogold labeling was performed with anti-GFP antibodies. Distribution of fusion proteins in the Golgi was expressed as a percentage of label observed for 15 individual stacks analyzed in different cells **(D)**, with counts of gold particles on the *cis*-side and *trans*-side after having divided Golgi in two domains. SV, secretory vesicle.

DISCUSSION

In eukaryotic cells, most proteins entering the secretory pathway are *N*-glycosylated with the transfer of an oligosaccharide precursor $Glc_3Man_9GlcNac_2$ from a membrane lipid dolichol carrier to an Asn residue in an Asn-X-Ser/Thr sequence on the newly synthesized polypeptide chains. This precursor is then modified in the ER and in the Golgi apparatus by specific glycosidases and glycosyltransferases to generate the variety of *N*-glycans found on glycoproteins.

The model that glycosidases and glycosyltransferases constituting the plant *N*-glycan processing machinery are organized in an assembly line is illustrated in Figure 11. With the exception of glucosidase II (GCSII), all glycosidases and glycosyltransferases involved in this assembly line have the same type II membrane protein topology with a short N-terminal CT, a TMD, and lumenal stem and catalytic domains. Even though the relative position of glycosyltransferases in the assembly line is known to govern in part the structure of *N*-glycans produced by the cell, the mechanisms allowing their selective retention in certain Golgi cisternae are still poorly understood, especially in plant cells.

In this study, we have analyzed the targeting of several *N*-glycosylation enzymes and found that they are located in the ER and/or in the Golgi in good agreement with their position in the *N*-glycan maturation pathway. We have also investigated the sequence responsible for the targeting of ManI, a type II membrane protein located in the early Golgi and in the ER, and we have shown that the TMD length contains the essential targeting elements for this glycosidase. However both in silico analyses of plant glycosylation enzymes cloned so far and the characterization of a 13–amino acid N-terminal sequence responsible for GCSI retention in the ER indicate that TMD length is not always the only sorting determinant allowing the subcompartmentation of glycosidases and glycosyltransferases along the secretory system. Our results also exemplify that in silico analysis does not allow for a prediction of the location of type II membrane enzymes within the secretory pathway.

Plant *N*-Glycan Processing Enzymes Are Arranged along an Assembly Line in the Early Secretory Pathway

While there is general agreement that enzymes involved in the maturation of *N*-linked oligosaccharides are arranged in the correct sequence along the individual subcompartments of the animal secretory pathway (de Graffenried and Bertozzi, 2004; Young, 2004), very little data on the distribution of the homologous proteins from plants exist to date. This study represents a systematic elucidation of resident enzyme localization in the secretory pathway of plant cells. Although the results presented

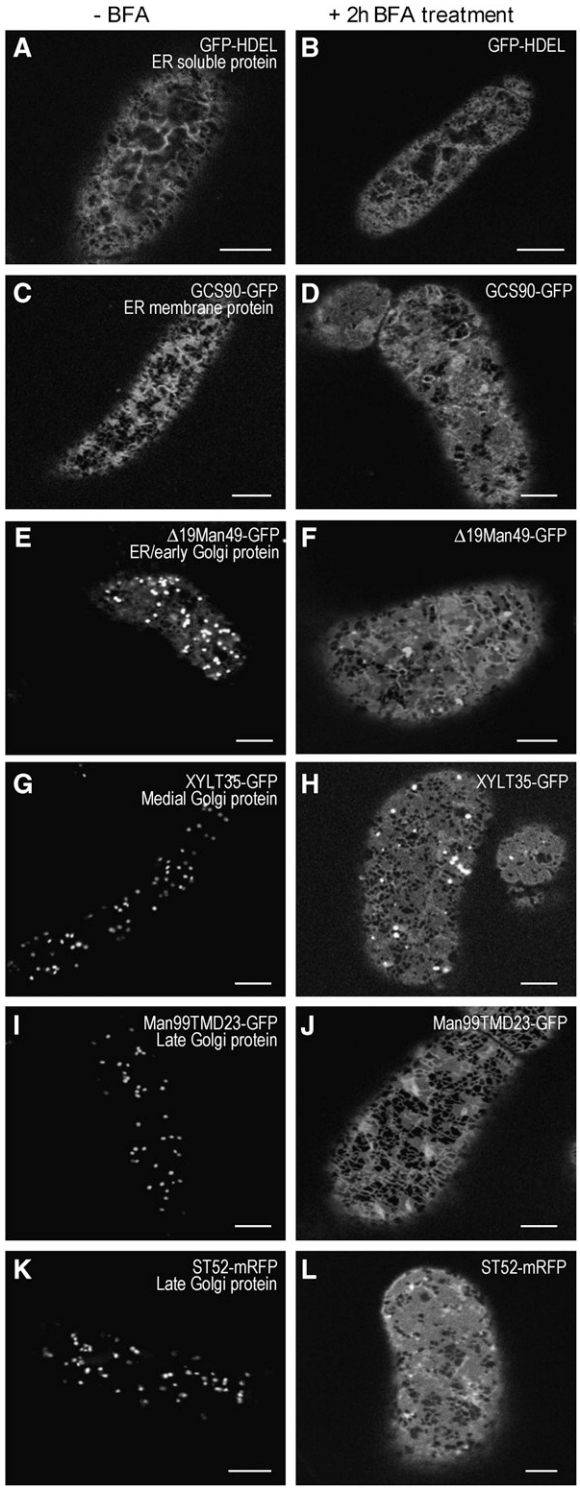

Figure 9. Effects of BFA on ER and/or Golgi Proteins in BY-2 Cells.

BY-2 cells expressing a soluble ER marker (GFP-HDEL; **[A]** and **[B]**) or a membrane ER marker (GCS90-GFP; **[C]** and **[D]**) display a typical fluorescence of the ER in the presence or absence of BFA. An ER and early Golgi marker (Δ19Man49-GFP; **[E]** and **[F]**), a medial Golgi marker (XYLT35-GFP; **[G]** and **[H]**), or late Golgi markers (Man99TMD23-GFP and ST52-GFP; **[I]** to **[L]**) highlight the ER and aggregates assimilated to Golgi clusters in the presence of BFA. Note that in all cases, the ER network often turns into fenestrated sheets of fluorescence. Bars = 8 μm.

here are in general agreement with those obtained in animal systems, some differences between secretory systems in these two eukaryotes are noteworthy.

Arabidopsis GCSI is located in the ER exclusively like its human counterpart (Hardt et al., 2003), and the CT in both proteins contains targeting information. In contrast with GCSI, we have found ManI and GNTI to be localized to both the Golgi and the ER. These two *N*-glycan maturation enzymes act sequentially during the production of mature *N*-glycans in plant and mammalian cells after a first trimming of the oligosaccharide precursor by GCSI and GCSII. The dual ER and Golgi localization of ManI and GNTI in plant cells contrasts with results obtained in mammals where these glycosylation enzymes are concentrated in the early Golgi compartments only. This difference could be a result of the different organization of the early secretory pathway in these organisms. Mammalian cells contain an intermediate compartment between ER and Golgi (known as ERGIC or VTC) that performs essential recycling functions (Ben-Tekaya et al., 2004). It is conceivable that this additional compartment allows animal cells to maintain a more specific distribution of ManI or GNTI.

Our results illustrate that there are at least two different classes of type II membrane proteins in the membranes of the early secretory pathway. The first class is exemplified in this study by ManI. In this case, we have shown that the TMD acts as a targeting sequence holding the protein in the ER and *cis*-Golgi compartments based on the length of hydrophobic TMDs. In a second population illustrated by GCSI, the TMD acts as a general anchor, and additional mechanisms, depending on signals contained in the CT, would locate these type II membrane proteins preferentially in the ER. In the latter case, we suggest, as it has been proposed by Hanton et al. (2005), that additional sequences, preferentially located in the CT on some type II membrane protein, are dominant over TMD length in determining protein targeting.

XYLT, a glycosyltransferase acting later in the maturation of *N*-glycans, has been localized almost exclusively to the medial Golgi apparatus (Pagny et al., 2003), again in keeping with the assembly line model. Interestingly, under the conditions used in this study, we cannot detect any of the XYLT-GFP fusion protein in the ER, which contrasts with the results obtained with ManI-GFP and GNTI-GFP. Assuming that XYLT-GFP continuously recycles through the ER, as has been shown for the *trans*-Golgi marker ST52-GFP (Brandizzi et al., 2002b), we have to postulate that the resident time of the protein in the ER is too short to allow for the accumulation of significant fluorescence signal in this compartment or that only a small fraction of XYLT-GFP actually recycles back to the ER.

In summary, all *N*-glycan processing enzymes of plants whose intracellular localization has been studied to date conform to the assembly line model in that their position within the organelles of the secretory pathway mirrors their position in the biochemical

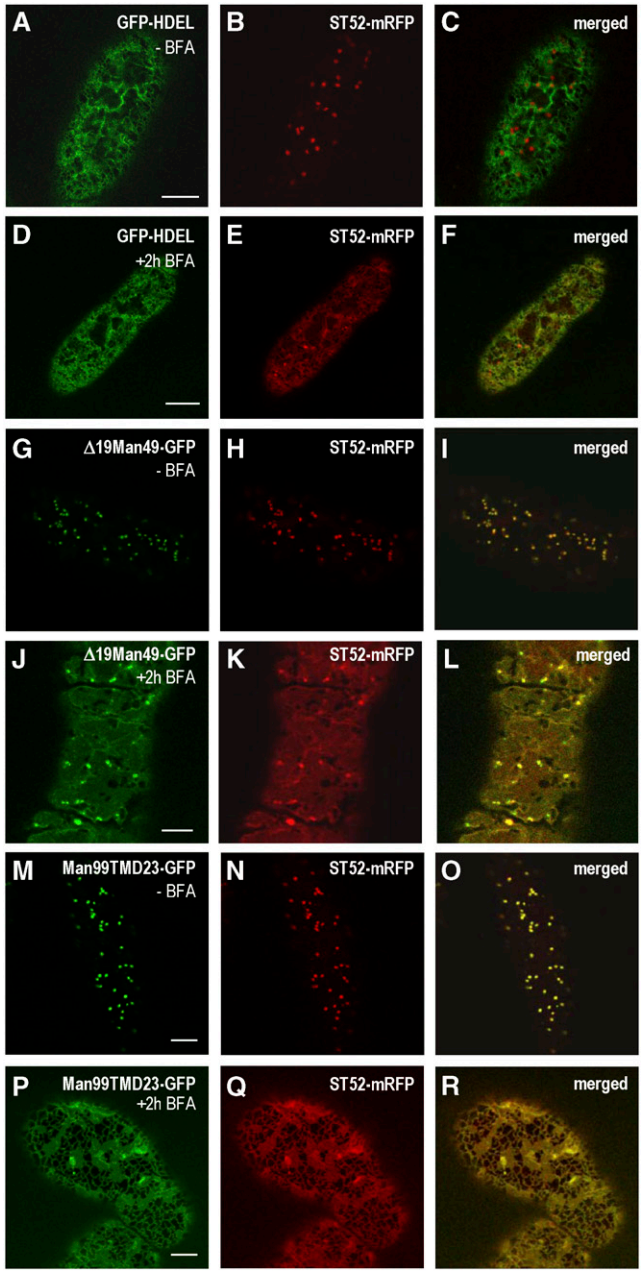

Figure 10. BFA Induces the Simultaneous Redistribution of Both Early and Late Golgi Markers into the ER and Golgi Clusters.

BY-2 cells coexpressing GFP-HDEL (**[A]** to **[F]**), Δ19Man49-GFP (**[G]** to **[L]**), or Man99TMD23-GFP (**[M]** to **[R]**) with ST52-mRFP were analyzed in the absence (**[A]** to **[C]**, **[G]**, **[H]**, and **[M]** to **[O]**) or presence (**[D]** to **[F]**, **[J]** to **[L]**, and **[P]** to **[R]**) of BFA (50 $\mu g \cdot mL^{-1}$).

pathway that results in complex *N*-linked oligosaccharides. While the precise distribution of enzyme activities in plants may not always match that found in animal systems, the general sequential arrangement of the enzymes is the same. As a corollary, it is now possible to use enzymes of the plant *N*-glycan maturation pathway as markers for the different subcompartments in the secretory pathway of plant cells. These new tools should also allow us to study the transport processes involved in movement of secretory cargo from the ER to the plasma membrane or to the vacuoles in greater detail. Furthermore, the differential localization of plant glycosyltransferases within the Golgi and the possibility to resolve at the light microscopy level the intra-Golgi targeting of these new markers offer a simple way to identify where the subset of cisternae a protein of interest goes.

Subcompartmentation of ManI Is Related to Its TMD Length

For mammalian cells, several models have been proposed to explain how type II membrane proteins are retained at different levels within the Golgi. According to the kin recognition model (Nilsson et al., 1993b), aggregation of *N*-glycan maturation enzymes by homo/hetero-oligomerization would prevent the resulting large complexes from being delivered to secretory vesicles and ongoing forward transport downstream in the secretory pathway. One of the first reported cases of this type of association involved ManII and GNTI, two glycosylation enzymes located in the medial-Golgi and acting sequentially in mammalian *N*-glycan maturation (Nilsson et al., 1994). It should be noted that this model originally assumes the presence of stable Golgi cisternae and the anterograde flow of secretory cargo via vesicular shuttles (Nilsson et al., 1993b). To fit with the cisternal progression/maturation concept, the kin recognition model would have to be modified to allow for the oligomeric complexes to be preferentially packaged into retrograde vesicles (Füllekrug and Nilsson, 1998). A second model, the lipid bilayer model (Bretscher and Munro, 1993) proposes that the fit between the length of TMD of glycan maturation enzymes and the thickness of the lipid bilayer of each organelle membrane determines the localization because each organelle has its specific membrane lipid composition and consequently its own thickness (Morré and Mollenhauer, 1974; Hartmann and Benveniste, 1987; Lynch, 1993; Moreau et al., 1998). Comparisons revealed that the length of Golgi protein TMD were on average five amino acids shorter than those of plasma membrane proteins (Masibay et al., 1993; Munro, 1995a). Several examples are in favor of this model. An increase of the length of the TMD of rat α-2,6-ST and bovine β-1,4-galactosyltransferase reduced the Golgi retention of these glycosyltransferases. In addition, a synthetic type I TMD made of 17 Leu residues resulted in Golgi retention of the lymphocyte surface antigen CD8 extracellular domain, whereas a 23-Leu TMD was found in increased amounts at the cell surface (Munro, 1991, 1995b; Masibay et al., 1993). Furthermore, incremental increases in the length of the 18–amino acid α-2,6-ST TMD by insertion of one to nine hydrophobic amino acids also resulted in increased cell surface expression of similar α-2,6-ST lysosyme chimeras, while the decrease in the length of a plasma membrane protein TMD led to its increased retention in the Golgi (Munro, 1995b).

In plant cells, preliminary data in favor of a subcompartmentation of membrane proteins along the endomembrane system related to the TMD length was obtained by varying the length of TMDs in two type I membrane proteins fused to GFP (Brandizzi

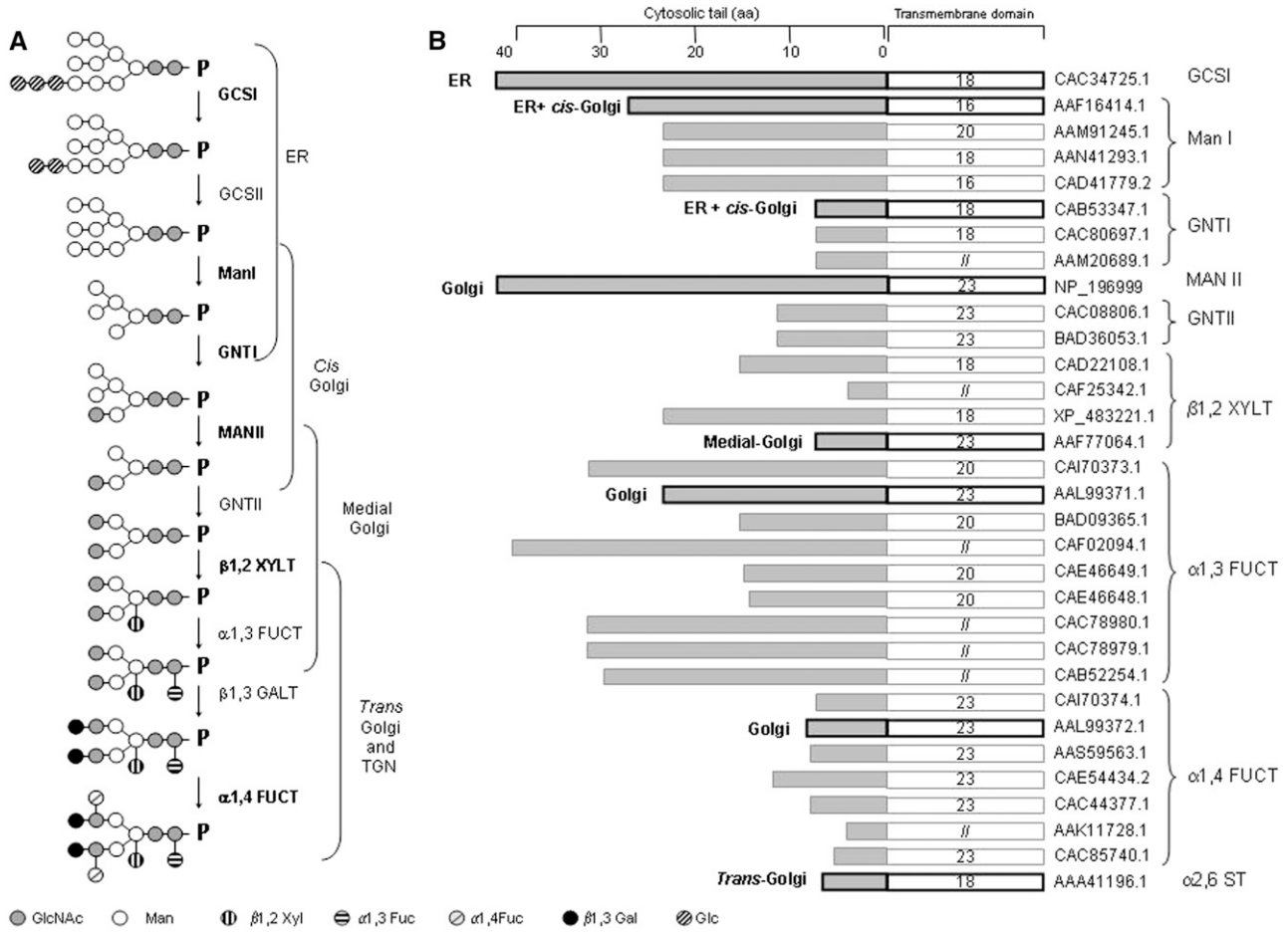

Figure 11. Comparison of CT and TMD Length for Plant *N*-Glycosylation Enzymes.

(A) Processing of *N*-linked glycans in the ER and Golgi apparatus of plant cells. A precursor oligosaccharide ($Glc_3Man_9GlcNAc_2$) assembled onto a lipid carrier is transferred on specific Asn residues of the nascent polypeptide (P). This precursor is then modified by glycosidases and glycosyltransferases mainly in the ER and the Golgi apparatus during the transport of the glycoprotein downstream the secretory pathway. Glycosidases and glycosyltransferases responsible for plant *N*-glycan maturation and their localization in the biochemical processing pathway are indicated. *N*-glycan processing enzymes whose intracellular localization has been studied to date (in boldface characters; this study; Pagny et al., 2003; Strasser et al., 2006; C. Saint-Jore-Dupas, M.C. Kiefer-Meyer, and V. Gomord, unpublished data) confirm the assembly line concept in that their position within the organelles of the secretory pathway (at the right) mirrors their position in the biochemical pathway (at the left).

(B) CT and TMD length of *N*-glycan processing enzymes that have been cloned from different plant species. Accession numbers are indicated at the right of each schematic representation. For each membrane protein, the position and the size of the TMD were estimated from TmHMM_v2 software (http://www.cbs.dtu.dk/services/TMHMM/). For some of the proteins, the probability to define the position of the TMD is below 50% (//). Boxes outlined in bold correspond to *N*-glycan processing enzymes whose intracellular localization has been studied to date by confocal and/or electronic microscopy. GNTII, *N*-acetylglucosaminyltransferase II; β1,2XYLT, β1,2 xylosyltransferase; α1,3 FucT, α1,3 fucosyltransferase; α1,4 FucT, α1,4 fucosyltransferase; β1,3 GalT, β1,3 galactosyltransferase.

et al., 2002a). First, the human lysosomal membrane protein LAMP1 containing a 23–amino acid TMD was fused to GFP and was expressed in tobacco leaves. The fusion was located in the plasma membrane. By contrast, when the TMD was shortened to 20 and 17 amino acids, the GFP chimeras were localized to the Golgi and ER membranes, respectively. Secondly the 19–amino acid TMD of the vacuolar sorting receptor BP80 targeted GFP to the Golgi, whereas a lengthened TMD of 22 amino acids targeted GFP to the plasma membrane.

In this study, we have investigated whether the TMD length of the type II membrane protein ManI could affect its subcompartmentation in the Golgi. In particular, we have increased the TMD length from 16 to 23 amino acids by duplicating the last seven amino acids of this domain. In contrast with their homologues containing a 16–amino acid TMD, which were located in the ER and the *cis*-half of the Golgi apparatus, chimeric proteins with a 23–amino acid TMD were localized exclusively to the Golgi and more precisely in the *trans*-half of the Golgi stacks. Together with

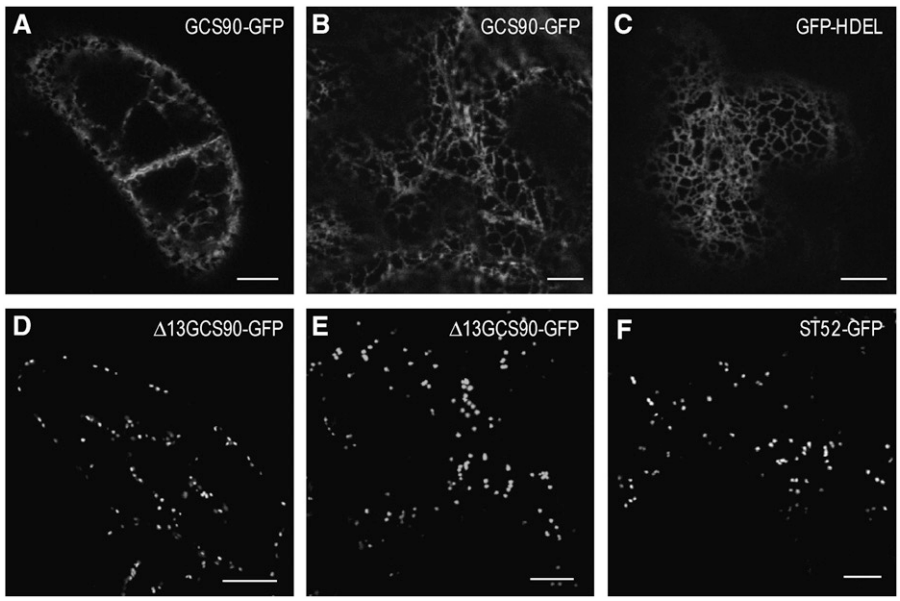

Figure 12. The TMD Does Not Always Carry the Major Targeting Information: Evidence from GCSI Targeting to the ER.

(A) to **(C)** In BY-2 cells, GCS90-GFP **(A)** highlighted the ER like the full-length GFP fusion GCSI-GFP (Figure 2G) and the ER marker GFP-HDEL (Figures 2D and 2E). In *Nicotiana* leaf epidermal cells, GCS90-GFP **(B)** also shows the same network pattern as GFP-HDEL **(C)**. Bars = 8 μm.
(D) to **(F)** After deletion of the first 13 amino acids of the CT of GCS90-GFP, Δ13GCS90-GFP localized in the Golgi in BY-2 cells **(D)** and *Nicotiana* leaf epidermal cells **(E)** as observed for XYLT or ST52-GFP/mRFP (Figures 6E and 6F, respectively) . Bars = 16 μm in **(D)** and **(E)** and 8 μm in **(F)**.

our results demonstrating that the TMD is sufficient to confer an identical localization as the full-length protein ManI, our data suggest that the length of the TMD is a crucial factor for precise positioning of this type II membrane protein within the Golgi stacks and the ER. Thus, protein–lipid interactions are expected to play a key role in ManI targeting within the secretory system.

Interestingly, these results also clearly point out differences in TMD length requirements in the targeting of type I and type II membrane proteins in the plant secretory system. Indeed, the 23–amino acid TMD of XYLT (Dirnberger et al., 2002; Pagny et al., 2003) or the 22–amino acid TMD of ManII (Strasser et al., 2006) targets GFP to the Golgi only. In addition, here, ManI with a lengthened TMD (23 amino acids) is also detected exclusively in the Golgi. By contrast, the 23–amino acid TMD of a type I membrane protein and the lengthened 22–amino acid TMD of BP80 target GFP to the plasma membrane in Brandizzi et al. (2002a). The TMD length requirements for a membrane protein to stay in a membrane with a given thickness might depend on the topology of the protein (type I or type II). While these experiments clearly demonstrate the role of TMD length in ManI protein targeting, we could also show that other enzymes require other signals for proper localization. For example, contradicting the trend to longer TMDs in the later parts of the Golgi, the ST52-GFP fusion with an 18–amino acid TMD is found further downstream in the *trans*-Golgi (Boevink et al., 1998; Wee et al., 1998) than the XYLT35-GFP fusion with a 23–amino acid TMD (Pagny et al., 2003).

Even in the situation illustrated here with GCSI, whose TMD is one of the shortest identified so far for a plant glycosylation enzyme and allows for a localization in the ER, we now show that additional information contained in the CT are required for proper targeting. Thus, in silico analyses and mutagenesis studies performed on GCSI are not consistent with TMD length as the only signal for compartmentation of glycosylation enzymes in the plant secretory system. In other words, while the TMD length plays a key role for ManI targeting in the ER and the *cis*-Golgi, results obtained with GCSI illustrate that specific localization of some membrane proteins in the ER or Golgi membranes could also depend on both protein–lipid (via the TMD) and protein–protein (via special sorting motifs) interactions. The identification of cytosolic partners, such as Golgi matrix proteins or cytoplasmic regulators, should help us to explain mechanisms involved in this second model for partitioning the *N*-glycan maturation enzymes along the plant secretory pathway.

The large collection of enzymes localizing to different levels in the Golgi has allowed us to test the question whether all cisternae within the Golgi stack fuse with the ER in response to treatment with the fungal toxin BFA. Indeed the Man-GFP fusions containing either a 16– or 23–amino acid TMD and ST52-mRFP all moved back to the ER or in Golgi clusters over a 2-h time-course experiment with BFA. These conclusions are consistent with previously published results (Nebenführ et al., 2002; Ritzenthaler et al., 2002).

Conclusions

We have demonstrated that the enzymes of the *N*-glycan processing pathway are spatially arranged so that they form an assembly line where individual enzymes act sequentially on their glycoprotein substrates. The length of the TMD can act as a key

signal in targeting some glycosylation enzymes to their proper location within the secretory pathway, as exemplified here with ManI. However, we have also discovered instances where additional targeting signals located in the CT of type II membrane proteins must be operating, for example, to prevent loss of GCSI from the ER. Further studies will use GCSI as a model to investigate the mechanisms that plant cells employ to translate these signals into a specific subcellular localization.

METHODS

Constructs

All ManI fusion constructs were derived from the full-length GFP fusion (here called ManI-GFP) originally described by Nebenführ et al. (1999). First, a linker containing an *Aat*II restriction site was introduced between the ManI and the GFP coding regions. In combination with the native *Aat*II site near the end of the predicted stem region, this allowed for simple removal of the catalytic domain to yield Man99-GFP.

Second, to facilitate the removal of specific segments of the N-terminal region, three new restriction sites were introduced by PCR mutagenesis: one *Nhe*I site immediately behind the start codon, one *Spe*I site at codons 21 and 22, and another *Aat*II site at codons 50 and 51. The integrity of the modified construct was confirmed by sequencing. In this new construct, the CT could be removed with *Nhe*I and *Spe*I to give Δ19CTManI-GFP, while an *Aat*II digest would remove the entire lumenal part of ManI to yield Man49-GFP. Combination of the two procedures resulted in Δ19CTMan49-GFP. Finally, forward (5′-GATCCTTGGGAATGCTTGCTCTGCTCTTCATCGTTTTCGTTTGTGTCTCTTTCGTTTTCTGGGACCGTCAAA-3′) and reverse (5′-CTAGTTTGACGGTCCCAGAAAACGAAAGAGACACAAACGAAAACGATGAAGAGCAGAGCAAGAGCATTCCCAAG-3′) oligonucleotides encoding the 18 amino acids of the TMD domain with a start codon were synthesized, fused, and subcloned into the pBLTI121 binary vector containing the GFP without any start codon (M.C. Kiefer-Meyer and V. Gomord, unpublished data) to give ΔCTMan49-GFP. The same strategy has been used to generated MAAMan49-GFP using forward (5′-GATCCTTGGGAATGGCTGCTGCTCTTGCTCTGCTCTTCATCGTTTTCGTTTGTGTCTCTTTCGTTTTCTGGGACCGTCAAA-3′) and reverse (5′-CTAGTTTGACGGTCCCAGAAAACGAAAGAGACACAAACGAAAACGATGAAGAGCAGAGCAAGAGCAGCAGCCATTCCCAAG-3′) primers.

Third, a longer TMD region was introduced in a two-step PCR mutagenesis of the modified ManI described above. In the first step, the *Aat*II site following the TMD was replaced with a *Bsp*EI site. In the second step, a long PCR primer was used to duplicate the last seven amino acids of the predicted TMD to yield ManTMD23-GFP. Finally, the catalytic domain of this construct was removed with *Aat*II to give Man99TMD23-GFP.

All cloning steps described above were performed in pBluescript SK+. The finished expression cassettes (including a double 35S promoter and a Nos terminator) were then moved to pBIN20 (Hennegan and Danna, 1998).

To obtain the plant binary vector encoding ST-mRFP, GFP was replaced with mRFP (provided by Roger Tsien) in pVKH18En6 ST-GFP (Saint-Jore et al., 2002). ST-mRFP expression is under control of 6x tandemly repeated CaMV 35S promoters.

GNTI-GFP and GNT38-GFP were amplified by PCR using the *Nicotiana tabacum* cDNA encoding N-GNTI as template (Strasser et al., 1999). Reverse primers 5′-GGTCACTAGTATCTTCATTTCCGAGTTG-3′ and 5′-GGTCACTAGTGCGATCTGCATATTCTGACTG-3′ were used for PCR with the forward primer 5′-AACGTCTAGAATGAGAGGGTACAAGTTTTGC-3′ to amplify the GNTI and the N-terminal 38–amino acid end of the GNTI to obtain GNTI-GFP and GNT38-GFP, respectively. To express GCSI-GFP, the total cDNA was amplified by PCR using *Arabidopsis thaliana* cDNA cloned as by Boisson et al. (2001), fused at the N-terminal end of GFP, and subcloned in pBLTI121 (Pagny et al., 2003). Then, the first 90 amino acids were amplified by PCR with forward (5′-CGGGGTACCCCATGACCGGAGCTAGCCGT-3′) and reverse (5′-GACTAGAAAAGGAGTGATAACCCT-3′) primers and subcloned in the *Spe*I restriction site located at the 5′ end of GFP contained in the pBLTI121 binary vector to give GCS90-GFP. In the same way, the 90 amino acids deleted of the first 13 amino acids were amplified by PCR with forward primer (5′-CGGGGTACCCCATGAAATCATCATCATTATCTCCC-3′) and the same reverse primers as above to give Δ13GCS90-GFP.

Agrobacterium-Mediated Tobacco BY-2 Cell Transformation

pVKH18En6-mRFP, PBLTI121-GFP, and pBIN20-GFP-fusions were transferred into *Agrobacterium tumefaciens* (strain GV3101 pMP90; Koncz and Schell, 1986) by heat shock. Transgenic *Agrobacterium* were selected onto YEB medium (per liter, 5 g beef extract, 1 g yeast extract, 5 g sucrose, and 0.5 g $MgSO_4$ $7H_2O$) containing kanamycin (100 $\mu g \cdot mL^{-1}$) and gentamycin (10 $\mu g \cdot mL^{-1}$) and were used to transform *N. tabacum* (cv BY-2) cells, as described by Gomord et al. (1998). Transformed tobacco cells were selected in the presence of kanamycin (100 $\mu g \cdot mL^{-1}$) for PBLTI121-GFP and pBIN20-GFP fusions or hygromycin (40 $\mu g \cdot mL^{-1}$) for pVKH18En6-mRFP and cefotaxime (250 $\mu g \cdot mL^{-1}$). For the double transformants coexpressing GFP and mRFP fusions, microcalli were first selected onto kanamycin plates and were then transferred onto hygromycin plates. After screening, calli expressing the GFP and or mRFP fusions were used to initiate suspension cultures of transgenic cells. Three- to four-day-old BY-2 suspension-cultured cells were used for experiments.

Agrobacterium-Mediated Transient Expression in *N. tabacum*, *Glycine max*, and *Solanum lycopersicum*

Agrobacterium was cultured at 28°C until the stationary phase (~20 h), washed, and resuspended in infiltration medium (50 mM MES, pH 5.6, 0.5% glucose [w/v], 2 mM Na_3PO_4, and 100 μm acetosyringone from 10 mM stock in absolute ethanol [Sigma-Aldrich]) (Saint-Jore et al., 2002). The bacterial suspension was pressure injected into the abaxial epidermis of *N. tabacum*, *G. max*, or *S. lycopersicum* leaves using a 1-mL plastic syringe by pressing the nozzle against the lower leaf epidermis (Neuhaus and Boevink, 2001). The plants were incubated for 3 d at 20 to 25°C unless specified in the figure legend. For tomato and soybean, the same transformation procedure was followed, but the cells were observed after 2 d.

Drug Treatments

Tobacco cells were incubated in 30 $\mu g \cdot mL^{-1}$ cycloheximide for 2 h or 50 $\mu g \cdot mL^{-1}$ BFA for 2 h before confocal analysis (from 10 $mg \cdot mL^{-1}$ stock in DMSO [Sigma-Aldrich]).

Confocal Laser Scanning Microscopy

Cells expressing GFP/mRFP fusions were imaged using a Leica TCS SP2 AOBS confocal laser scanning microscope. Single-color imaging of GFP was done using a 488-nm argon ion laser line, and the fluorescence was recorded by a photomultiplier set up for 493 to 538 nm. Dual-color imaging of cells coexpressing GFP and mRFP was performed using simultaneously a 488-nm argon ion laser line and a HeNe 543-nm laser line. Fluorescence signals were separated using an acousto-optical beam splitter, and GFP emission was detected in photomultiplier 2 (493 to 538 nm), whereas mRFP was collected in photomultiplier 3 (580 to 620 nm). The power of each laser line, the gain, and the offset were

identical for each experiment so that the images were comparable. Appropriate controls were performed to exclude the possibility of cross-talk between the two fluorochromes before the image acquisition.

Sample Preparation, Immunogold Labeling, and Electron Microscopy

Immunolabeling was performed on cryosections of 3-d-old BY-2 suspension-cultured cells fixed in a mixture of 2% formaldehyde and 2% glutaraldehyde for 16 h, embedded in 12% gelatin, and infiltrated with 2.3 M sucrose (M.-L. Follet-Gueye and A. Driouich, unpublished data). The cells were then frozen in liquid nitrogen and sectioned at −120°C (Leica UCT).

Grids were floated in successive solutions at room temperature for 2 min. They were first incubated in PBS buffer containing 0.1% glycin (w/v) to inactivate residual fixative. The grids were blocked in PBS buffer with 1% BSA (w/v) and then incubated with the anti-GFP antibodies diluted 1:100 in blocking buffer for 30 min. After washing in PBS buffer, the grids were blocked in normal goat serum (NGS5; British Biocell International) 1:30 in PBS buffer containing 0.1% BSA (w/v). After incubation with the secondary antibody (10 nm EM gold conjugates, goat anti-rabbit IgG; British Biocell International) diluted 1:25 in blocking buffer for 30 min, the grids were incubated with 1% glutaraldehyde (v/v) in PBS for 5 min and finally washed in water. The specimen were stained for 5 min with 2% (w/v) cold methyl cellulose containing 0.4% (w/v) uranyl acetate, pH 4.0, and observed with a transmission electron microscope (Tecnai 12, 80 kV; FEI-Philips).

Accession Numbers

Sequence data of the genes from this article can be found in the GenBank/EMBL data libraries under the following accession numbers and Arabidopsis Genome Initiative locus identifiers: AF126550 (*G. max* ManI; Nebenführ et al., 1999), AF272852/At5g55500 (*Arabidopsis* XYLT; Pagny et al., 2003), NTY16832 (*N. tabacum* GNTI; Strasser et al., 1999), and AJ278990/At1g67490 (*Arabidopsis* GCSI; Boisson et al., 2001).

Supplemental Data

The following materials are available in the online version of this article.

Supplemental Table 1. Additional Data in Complement to Figure 11.

Supplemental Table 2. Transmembrane Domain Length Analysis.

ACKNOWLEDGMENTS

This work was supported by the Université de Rouen, the Centre National de Recherche Scientifique, and by the Ministère de la Jeunesse, de l'Education Nationale et de la Recherche (ACI Jeunes chercheurs 02-2-0486) for a postdoctoral grant to C.S-.J-.D. This work was also supported by a grant from the National Science Foundation to A.N. (MCB 0416931). We thank M.-C. Kiefer-Meyer and F. Brandizzi for making the binary plasmid containing sGFP and ST-mRFP fusion. We also thank those referees whose anonymity did not prevent them from supporting this work by putting forward a set of constructive criticisms and most useful suggestions. All the microscopy experiments were performed at the ''Plateforme d'Imagerie cellulaire de Haute-Normandie'' at the Université de Rouen.

Received July 21, 2005; revised August 31, 2006; accepted November 2, 2006; published November 30, 2006.

REFERENCES

Andreeva, A.V., Kutuzov, M.A., Evans, D.E., and Hawes, C. (1998). The structure of the Golgi apparatus: A hundred year of questions. J. Exp. Bot. **49,** 1281–1291.

Ben-Tekaya, H., Miura, K., Pepperkok, R., and Hauri, H.P. (2004). Live imaging of bidirectional traffic from the ERGIC. J. Cell Sci. **118,** 357–367.

Boevink, P., Oparka, K., Santa Cruz, S., Martin, B., Betteridge, A., and Hawes, C. (1998). Stacks on tracks: The plant Golgi apparatus traffics on an actin/ER network. Plant J. **15,** 441–447.

Boisson, M., Gomord, V., Audran, C., Berger, N., Dubreucq, B., Granier, F., Lerouge, P., Faye, L., Caboche, M., and Lepiniec, L. (2001). *Arabidopsis* glucosidase I mutants reveal a critical role of N-glycan trimming in seed development. EMBO J. **20,** 1010–1019.

Brandizzi, F., Frangne, N., Marc-Martin, S., Hawes, C., Neuhaus, J.-M., and Paris, N. (2002a). The destination for single-pass membrane proteins is influenced markedly by the length of the hydrophobic domain. Plant Cell **14,** 1077–1092.

Brandizzi, F., Snapp, E., Roberts, A., Lippincott-Schwartz, J., and Hawes, C. (2002b). Membrane protein transport between the ER and Golgi in tobacco leaves is energy dependent but cytoskeleton independent: Evidence from selective photobleaching. Plant Cell **14,** 1293–1309.

Bretscher, M.S., and Munro, S. (1993). Cholesterol and the Golgi apparatus. Science **261,** 1280–1281.

Campbell, R.E., Tour, O., Palmer, A.E., Steinbach, P.A., Baird, G.S., Zacharias, D.A., and Tsien, R.Y. (2002). A monomeric red fluorescent protein. Proc. Natl. Acad. Sci. USA **99,** 7877–7882.

Colley, K.J. (1997). Golgi localization of glycosyltransferases: More questions than answers. Glycobiology **7,** 1–13.

Coutinho, P.M., Stam, M., Blanc, E., and Henrissat, B. (2003). Why are there so many carbohydrate-active enzyme-related genes in plants? Trends Plant Sci. **8,** 563–565.

de Graffenried, C.L., and Bertozzi, C.R. (2004). The roles of enzyme localization and complex formation in glycan assembly within the Golgi apparatus. Curr. Opin. Cell Biol. **16,** 356–363.

Dirnberger, D., Bencur, P., Mach, L., and Steinkellner, H. (2002). The Golgi localization of *Arabidopsis thaliana* beta1,2-xylosyltransferase in plant cells is dependent on its cytoplasmic and transmembrane sequences. Plant Mol. Biol. **50,** 273–281.

Driouich, A., and Staehelin, L.A. (1997). The plant Golgi apparatus: Structural organization and functional properties. In The Golgi Apparatus, E.G. Berger and J. Roth, eds (Basel, Switzerland: Birkhauser Verlag), pp. 275–301.

Dupree, P., and Sherrier, D.J. (1998). The plant Golgi apparatus. Biochim. Biophys. Acta **1404,** 259–270.

Essl, D., Dirnberger, D., Gomord, V., Strasser, R., Faye, L., Glössl, J., and Steinkellner, H. (1999). The N-terminal 77 amino acids from tobacco N-acetylglucosaminyltransferase I are sufficient to retain a reporter protein in the Golgi apparatus of *Nicotiana benthamiana* cells. FEBS Lett. **453,** 169–173.

Fitchette, A.C., Cabanes-Macheteau, M., Marvin, B., Satiat-Jeunemaitre, B., Gomord, V., Lerouge, P., Faye, L., and Hawes, C. (1999). Biosynthesis and immunolocalization of Lewis-a-containing N-glycans in the plant cells. Plant Physiol. **121,** 333–334.

Fitchette, A.C., Gomord, V., Chekkafi, A., and Faye, L. (1994). Distribution of xylosylation and fucosylation in the plant Golgi apparatus. Plant J. **5,** 673–682.

Füllekrug, J., and Nilsson, T. (1998). Protein sorting in the Golgi complex. Biochim. Biophys. Acta **1404,** 77–84.

Giraudo, C.D., and Maccioni, H.J.F. (2003). Endoplasmic reticulum export of glycosyltransferases depends on interaction of a cytoplasmic dibasic motif with Sar1. Mol. Biol. Cell **14,** 3753–3766.

Gleeson, P.A. (1998). Targeting of proteins to the Golgi apparatus. Histochem. Cell Biol. **109,** 517–532.

Gomord, V., Fitchette, A.C., Denmat, L.A., Michaud, D., and Faye, L. (1998). Production of foreign proteins in tobacco cell suspension culture. In Methods in Molecular Biotechnology, Vol. 3, C. Cunningham and A.J.R. Porter, eds (Totowa, NJ: Humana Press), pp. 155–164.

Grove, S.N., Brecker, C.E., and Morré, D.J. (1968). Cytomembrane differentiation in the endoplasmic reticulum-Golgi apparatus-vesicle complex. Science **161,** 171–173.

Hanton, S.L., Renna, L., Bortolotti, L.E., Chatre, L., Stefano, G., and Brandizzi, F. (2005). Diacidic motifs influence the export of transmembrane proteins from the endoplasmic reticulum in plant cells. Plant Cell **17,** 3081–3093.

Hardt, B., Kalz-Füller, B., Aparicio, R., Völker, C., and Bause, E. (2003). (Arg)3 within the N-terminal domain of glucosidase I contains ER targeting information but is not required absolutely for ER localisation. Glycobiology **13,** 159–168.

Hartmann, M.A., and Benveniste, P. (1987). Plant membrane sterols: Isolation, identification and biosynthesis. Methods Enzymol. **148,** 632–650.

Hawes, C. (2005). Cell biology of the plant Golgi apparatus. New Phytol. **165,** 29–44.

Hawes, C., and Satiat-Jeunemaitre, B. (2005). The plant Golgi apparatus – Going with the flow. Biochim. Biophys. Acta **1744,** 93–107.

Hennegan, K.P., and Danna, K.J. (1998). pBIN20: An improved binary vector for *Agrobacterium*-mediated transformation. Plant Mol. Biol. Rep. **16,** 129–131.

Idgoura, S.A., Herscovics, A., Lal, A., Moremen, K.W., Morales, C.R., and Hermo, L. (1999). α-Mannosidases involved in N-glycan processing show cell specificity and distinct sub-compartmentalization within the Golgi apparatus of cells in the testis and epididymis. Eur. J. Cell Biol. **78,** 441–452.

Koncz, C., and Schell, J. (1986). The promoter of T-DNA gene 5 controls the tissue-specific expression of chimeric genes carried by a novel type of *Agrobacterium* binary vector. Mol. Gen. Genet. **204,** 383–396.

Lainé, A.C., Gomord, V., and Faye, L. (1991). Xylose-specific antibodies as markers of subcompartmentation of terminal glycosylation in the Golgi apparatus of sycamore cells. FEBS Lett. **295,** 179–184.

Lerouge, P., Cabanes-Macheteau, M., Rayon, C., Fitchette-Lainé, A.C., Gomord, V., and Faye, L. (1998). N-glycoprotein biosynthesis: Recent development and future trends. Plant Mol. Biol. **38,** 31–48.

Lynch, D.V. (1993). Sphingolipids. In Lipid Metabolism in Plants, T.S. Moore, ed (Boca Raton, FL: CRC Press), pp. 285–308.

Masibay, A.S., Balaji, P.V., Boeggeman, E.E., and Qasba, P.K. (1993). Mutational analysis of the Golgi retention signal of bovine β-1, 4-galactosyltransferase. J. Biol. Chem. **268,** 9908–9916.

Milland, J., Russell, S.M., Dodson, H.C., McKenzie, I.F., and Sandrin, M.S. (2002). The cytoplasmic tail of α-1,3-galactosyltransferase inhibits Golgi localization of the full length enzyme. J. Biol. Chem. **277,** 10374–10378.

Milland, J., Taylor, S.G., Dodson, H.C., McKenzie, I.F.C., and Sandrin, M.S. (2001). The cytoplasmic tail of α-1,2-fucosyltransferase contains a sequence for Golgi localization. J. Biol. Chem. **276,** 12012–12018.

Moreau, P., Hartmann, M.A., Perret, A.M., Sturbois-Balcerzak, B., and Cassagne, C. (1998). Transport of sterols to the plasma membrane of leek seedlings. Plant Physiol. **117,** 931–937.

Morré, D.J., and Mollenhauer, H.H. (1974). The endomembrane concept: A functional integration of endoplasmic reticulum and Golgi apparatus. In Dynamic Aspects of Plant Ultrastructure, A.W. Robards, ed (London: McGraw-Hill), pp. 84–137.

Munro, S. (1991). Sequences within and adjacent to the transmembrane segment of β-2,6-sialyltransferase specify Golgi retention. EMBO J. **10,** 3577–3588.

Munro, S. (1995a). A comparison of the transmembrane domains of Golgi and plasma membrane proteins. Biochem. Soc. Trans. **23,** 527–530.

Munro, S. (1995b). An investigation of the role of the transmembrane domain in Golgi protein retention. EMBO J. **14,** 4695–4704.

Munro, S. (1998). Localization of proteins to the Golgi apparatus. Trends Cell Biol. **8,** 11–15.

Nebenführ, A. (2002). Vesicle traffic in the endomembrane system: A tale of COPs, Rabs, and SNAREs. Curr. Opin. Plant Biol. **5,** 507–512.

Nebenführ, A., Gallagher, L.A., Dunahay, T.G., Frohlick, J.A., Mazurkiewicz, A.M., Meehl, J.B., and Staehelin, L.A. (1999). Stop-and-go movements of plant Golgi stacks are mediated by the acto-myosin system. Plant Physiol. **121,** 1127–1142.

Nebenführ, A., Ritzenthaler, C., and Robinson, D.G. (2002). Brefeldin A: Deciphering an enigmatic inhibitor of secretion. Plant Physiol. **130,** 1102–1108.

Nebenführ, A., and Staehelin, L.A. (2001). Mobile factories: Golgi dynamics in plant cells. Trends Plant Sci. **6,** 160–167.

Neuhaus, J.M., and Boevink, P. (2001). The green fluorescent protein (GFP) as a reporter in plant cells. In Plant Cell Biology: A Practical Approach, C.R. Hawes and B. Satiat-Jeunemaître, eds (Oxford, UK: Oxford University Press), pp. 127–142.

Nilsson, T., Hoe, M.H., Slusarewicz, P., Rabouille, C., Watson, R., Hunte, F., Watzele, G., Berger, E.G., and Warren, G. (1994). Kin recognition between medial Golgi enzymes in HeLa cells. EMBO J. **13,** 562–574.

Nilsson, T., Pypaert, M., Hoe, M.H., Slusarewicz, P., Berger, E.G., and Warren, G. (1993a). Overlapping distribution of two glycosyltransferases in the Golgi apparatus of HeLa cells. J. Cell Biol. **120,** 5–13.

Nilsson, T., Rabouille, C., Hui, N., Watson, R., and Warren, G. (1996). The role of the membrane spanning domain and stalk region of N-acetylglucosaminyltransferase I in retention, kin recognition and structural maintenance of the Golgi apparatus in HeLa cells. J. Cell Sci. **109,** 1975–1989.

Nilsson, T., Slusarewicz, P., Hoe, M.H., and Warren, G. (1993b). Kin recognition: A model for the retention of Golgi enzymes. FEBS Lett. **330,** 1–4.

Opat, A.S., Houghton, F., and Gleeson, P.A. (2000). Medial Golgi but not late Golgi glycosyltransferases exist as high molecular weight complexes. J. Biol. Chem. **275,** 11836–11845.

Osman, N., McKenzie, I.F.C., Mouhtouris, E., and Sandrin, M.S. (1996). Switching amino-terminal cytoplasmic domains of α(1,2)fucosyltransferase and α(1,3)galactosyltransferase alters the expression of H substance and Gal α(1,3)Gal. J. Biol. Chem. **271,** 33105–33109.

Pagny, S., Bouissonié, F., Sarkar, M., Follet-Gueye, M.L., Driouich, A., Schachter, H., Faye, L., and Gomord, V. (2003). Structural requirements for *Arabidopsis* β-1,2-xylosyltransferase activity and targeting to the Golgi. Plant J. **33,** 189–203.

Qian, R., Chen, C., and Colley, K.J. (2001). Location and mechanism of α-2,6-sialyltransferase dimmer formation. J. Biol. Chem. **276,** 28641–28649.

Rabouille, C., Hui, N., Hunte, F., Kleckbusch, R., and Berger, E.G. (1995). Mapping the distribution of Golgi enzymes involved in the construction of complex oligosaccharides. J. Cell Sci. **108,** 1617–1627.

Ritzenthaler, C., Nebenfuhr, A., Movafeghi, A., Stussi-Garaud, C., Behnia, L., Pimpl, P., Staehelin, L.A., and Robinson, D.G. (2002). Reevaluation of the effects of brefeldin A on plant cells using tobacco

Bright Yellow 2 cells expressing Golgi-targeted green fluorescent protein and COPI antisera. Plant Cell **14,** 237–261.

Roth, J. (1991). Localization of glycosylation sites in the Golgi apparatus using immunolabeling and cytochemistry. J. Electron Microsc. Tech. **17,** 121–131.

Runions, J., Brach, T., Külner, S., and Hawes, C. (2006). Photoactivation of GFP reveals protein dynamics within the endoplasmic reticulum membrane. J. Exp. Bot. **57,** 43–50.

Saint-Jore, C.M., Evins, J., Batoko, H., Brandizzi, F., Moore, I., and Hawes, C. (2002). Redistribution of membrane proteins between the Golgi apparatus and endoplasmic reticulum in plants is reversible and not dependent on cytoskeletal networks. Plant J. **29,** 661–678.

Saint-Jore-Dupas, C., Gomord, V., and Paris, N. (2004). Protein localization in the Golgi apparatus and the *trans*-Golgi network. Cell. Mol. Life Sci. **61,** 159–171.

Staehelin, L.A., and Moore, I. (1995). The plant Golgi apparatus: Structure, functional organisation and trafficking mechanisms. Annu. Rev. Plant Physiol. Plant Mol. Biol. **46,** 261–288.

Strasser, R., Mucha, J., Schwihla, H., Altmann, F., Glössl, J., and Steinkellner, H. (1999). Molecular cloning and characterisation of cDNA coding for β-1,2-N-acetylglucosaminyltransferase I (GlcNAc-TI) from *Nicotiana tabacum.* Glycobiology **9,** 779–785.

Strasser, R., Schoberer, J., Jin, C., Mucha, J., Glössl, J., Mach, L., and Steinkellner, H. (2006). Molecular cloning and characterisation of *Arabidopsis thaliana* Golgi α-mannosidase II, a key enzyme in the formation of complexN-glycans in plants. Plant J. **45,** 789–803.

Teasdale, R.D., and Jackson, M.R. (1996). Signal-mediated sorting of membrane proteins between the endoplasmic reticulum and the Golgi apparatus. Annu. Rev. Cell Dev. Biol. **12,** 27–54.

Trombetta, E.S., Fleming, K.G., and Helenius, A. (2001). Quaternary and domain structure of glycoprotein processing glucosidase II. Biochemistry **40,** 10717–10722.

Trombetta, E.S., Simons, J.F., and Helenius, A. (1996). Endoplasmic reticulum glucosidase II is composed of a catalytic subunit, conserved from yeast to mammals, and a tightly bound noncatalytic HDEL-containing subunit. J. Biol. Chem. **271,** 27509–27516.

Velasco, A., Hendricks, L., Moremen, K.W., Tulsiani, D.R.P., Touster, O., and Farquhar, M. (1993). Cell-type dependent variations in the subcellular distribution of α-mannosidase I and α-mannosidase II. J. Cell Biol. **122,** 39–51.

Wee, E.G.T., Sherrier, J., Prime, T., and Dupree, P. (1998). Targeting of active sialyltransferase to the plant Golgi apparatus. Plant Cell **10,** 1759–1768.

Young, W.W. (2004). Organization of Golgi glycosytransferases in membranes: Complexity via complexes. J. Membr. Biol. **198,** 1–13.

Yuasa, K., Toyooka, K., Fukuda, H., and Matsuoka, K. (2005). Membrane-anchored prolyl hydroxylase with an export signal from the endoplasmic reticulum. Plant J. **41,** 81–94.

Zerangue, N., Schwappach, B., Jan, Y.N., and Jan, L.Y. (1999). A new ER trafficking signal regulates the subunit stoichiometry of plasma membrane K (ATP) channels. Neuron **22,** 537–548.

Zerfaoui, M., Fukuda, M., Langlet, C., Mathieu, S., Suzuki, M., Lombardo, D., and Elbattari, A. (2002). The cytosolic and transmembrane domains of the β-1,6-N-acetylglucosaminyltransferase (C2GnT) function as a *cis* to medial/Golgi-targeting determinant. Glycobiology **12,** 15–24.

Zhang, G.F., and Staehelin, L.A. (1992). Functional compartmentation of the Golgi apparatus in plant cells. Plant Physiol. **99,** 1070–1083.